AD

Research and Development Technical Report
ECOM-0204-F

REFLECTIVITY-RAINFALL RELATIONSHIPS AND REFLECTIVITY VARIABILITY OBSERVED WITH A HYBRID VIDEO PROCESSOR

FINAL REPORT

by

E. J. Silha and E. A. Mueller

April 1971

ECOM

UNITED STATES ARMY ELECTRONICS COMMAND · FORT MONMOUTH, N.J.

Contract DAAB 07-69-C-0204
ILLINOIS STATE WATER SURVEY
at the
University of Illinois
Urbana, Illinois

TECHNICAL REPORT ECOM-0204-F

Reports Control Symbol
OSD-1366
December 1970

REFLECTIVITY-RAINFALL RELATIONSHIPS AND REFLECTIVITY VARIABILITY OBSERVED WITH A HYBRID VIDEO PROCESSOR

FINAL REPORT

1 February 1969 to 31 December 1970

Contract No. DAAB 07-69-C-0204

Prepared by

E.J. Silha and E. A. Mueller

ILLINOIS STATE WATER SURVEY
at the
University of Illinois
Urbana, Illinois

for

ATMOSPHERIC SCIENCES LABORATORY

U. S. ARMY ELECTRONICS COMMAND, FORT MONMOUTH, N. J.

ABSTRACT

A hybrid video processor was constructed for use in measuring rainfall in convective storms. After the processor was tested in the laboratory, it was used to collect data on two convective storms. Data were collected on 3 days, but on only one day did storm systems occur over the nearby raingage network where comparative rainfall data were available. The data were available. The data for these storms were analyzed to study relationships between reflectivity and rainfall. An attempt was made to correlate reflectivity with rainfall measured at the ground using a time-space displacement technique for the radar data. A comparison of total water accumulation is also made. Reflectivity variability described by a number of parameters was investigated.

LIST OF SYMBOLS & DEFINITIONS

L	Intensity level, the logarithm of intensity
L_{avg}	The measured average of intensity level
L_o	The true average intensity level
L_{est}	L_{avg} plus the correction for averaging the logarithm of intensity
I_{avg}	Average intensity
APMI	Automatic precipitation measurement indicator
FET	Field effect transistor
MOSFET	Metal-oxide field-effect transistor
IP	Illinois processor
WRSI	Weather radar signal integrator
RHI	Range height indicators
PPI	Plan position indicators
V	Volts
P_r	Received power
P_T	Transmitted power
Z	Radar reflectivity in mm^6/mm^3

TABLE OF CONTENTS

INTRODUCTION

This report presents various information on a hybrid video processor designed, developed, and tested in Illinois over the past 2 years. This processor combines analog integration with digital recording and was designed to obtain a large volume of digitized samples useful in radar-rainfall analyses. In the introduction various other means of obtaining signal integration electronically are discussed to illustrate the history of various other processors developed in the past 20 years. The technique of integration, the Illinois Preprocessor, the operations and data, and the analytical techniques employed are then presented. Results concerning the temporal variability of the resulting reflectivities and those from a limited radar-rainfall comparative study are discussed in detail, followed by conclusions and recommendations. The Appendix contains a very detailed discussion of the Illinois Processor.

The statistical behavior of radar reflectivities of meteorlogic targets is well known, and it is generally agreed that the average of a number of independent samples of the measured target intensity is needed to make an estimate of the true average target intensity. Since meteorological targets have a large dynamic range, logarithmic receivers are often used to observe them. Intensity level (L), the logarithm of intensity, varies in a statistically random manner also. To obtain a good estimate of the true average intensity level (L_0), a number of independent samples must be included in the average (L_{avg}). When a sufficient number of independent samples are included in L_{avg}, it converges to a value that is related to L_0 by the equation:

$$L_{avg} = L_0 - .25$$

The convergence limits, confidence limits, and relationships of Lavg and L_0 are described by Smith (1964). This statistical behavior of reflectivity requires that some sort of averaging be performed before reflectivity measurements can be used for quantative analysis.

Before the need for signal integration was completely understood, and to some extent later, radar data were collected by photographing range height indicators (RHI) and plan position indicators (PPI) of unprocessed video. This method provided some signal averaging by the cathode ray tube phospor and by the film. The inherent problems with this method are that the integration

process is not only difficult to control, but it is not reasonably described mathmatically so there is little quantitative measure of the integration process. This method is accurate to only ±5 db under the best conditions, as shown by Austin (1969). If radar is to be used as a quantitative tool in meteorology, some better means of measurement had to be devised.

Many approaches have been taken to improve measurement methods. Among the first were the range integrators. These were different types of low pass filters used in the video circuits to provide some range averaging at the expense of range resolution. In general, these devices provided an average composed of only a few samples. The range integrators also were used in conjunction with other equipment to obtain values for I_{avg} and L_{avg}. One such device was the area integrator developed by Farnsworth and Mueller (1956). This integrator used a low pass filter to average the range corrected video. The video was gain stepped and then constant areas over the study area (rain-gage network) where the video exceeded a preset threshold were summed. These areal blocks were given different weights according to the video gain step. The total count reflected the total rainfall over the network with no indication as to the distribution.

Another early means of performing the desired integration was the pulse integrator developed by Williams (1949). In this device a range of interest was gated from the video and fed to a "box-car generator". This circuit sampled the amplitude of the video at the range in question, and maintained this voltage for a period of time equal to the time between transmitter pulses. The box-car video was then passed through a low pass filter to derive a voltage proportional to the average signal level. The properties of the low pass filter and the radar pulse repetition frequency determined the number of samples in the average. The major drawback was that only one range at a time could be investigated. The present hybrid integrator in a sense is 50 pulse integrators operating simultaneously.

A later approach to integration used a quartz delay line. The radar transmitter was synchronized with the delay line recirculation rate. A portion of the new signal was added to a portion of the recirculated signal and the sum was recirculated through the delay line. The first of these integrators used an amplitude modulated RF carrier to drive the delay line. This type of integrator was limited in range resolution, and the number of samples used in the average was limited to about ten because of the instabilities inherent

in the analogue circuits. An improved version of this integrator using FM modulation reduced the stability problem, and more samples could be used in the average. Both of these approaches were used at MIT, as outlined by Austin (1969).

A variety of digital integrators has been used to observe meteorlogical targets. The Area Precipitation Measurement Indicator (APMI), developed by the United States Army Electronics Command, digitized the peak logarithmic video (maximum intensity level) in each range block. This device summed up to sixteen samples in each block, the number of samples summed being determined by operator controls. The sum was divided by shifting the binary word, and then the averaged value was stored in a rectangular coordinate array memory. The stored value was then displayed on a memory type cathode ray scope and photographed. Although the maximum intensity level in a range block may be a better estimator of L_0 for a small number of samples, Lavg is preferrable when more than ten samples are used in the average to obtain an estimate of L . Also an average containing more than 16 samples is needed in most quantative work. The APMI did provide immediate operational data, which was its purpose, but the need to photograph the data did not make the APMI easily adaptable as a research tool.

Another digital device, which was developed at M.I.T., (Austin, 1969), is a block integrator that uses a delay line as a memory. Logarithmic video in a range block is digitized and added to previous data from the same block. After the addition, the new sum is recirculated in the delay line. When the desired number of samples have been obtained, the data is normalized and range corrected. These data are then ready for display and recording. The need to synchronize the radar transmitter to the integrator delay line is inconvenient if there is need to use the integrator on more than one radar, or if there is need to use the radar for other purposes.

A more flexible device was developed at the South Dakota School of Mines and Technology by Smith and Boardman (1968). Logarithmic video is averaged in range blocks by a radar echo profiler manufactured by Arthur D. Little, Inc. The radar echo profiler is an analogue integrator similar to the device described by Lhermitte and Kessler (1965) and mentioned in the next section. The output of the profiler is digitized and either stored on digital magnetic tape or used by a PDP-8 general purpose computer to provide real time data.

INTEGRATION TECHNIQUE

The Illinois Processor described in the Appendix is similar to the Weather Radar Signal Integrator (WRSI) developed at the National Severe Storms Laboratory and described by Lhermitte and Kessler (1965). Both devices are hybrids, combining analog integration methods with digital recording methods. In both devices the integration is performed by a one dimensional array of contiguous range blocks. Each block is an exponential averaging analog circuit that is active only during one range time period.

The integration is performed in both processors by charging a memory capacitor through a resistor driven by the logarithmic video. The charge on the capacitor is a measure of L_{avg}. The WRSI uses a bipolar transistor to perform the analog gating which divides the range dimension into blocks. Since this is a unidirectional gate, a drain resistor is used to fix the discharging integration time; the charging integration time is controlled by another circuit. In the IP a field effect transistor (FET) performs the analog range gating. Since FET's are symmetrical, one circuit controls the total integration time.

The WRSI accomplishes readout by interleaving data collection and data conversion. The system timing is controlled by the radar PRF. As data is converted it is stored in a buffer and then recorded when the buffer is filled. The preprocessor has separate timing for data acquisition and data recording. The acquisition timing is controlled by the radar PRF. The recording timing is controlled by the recording device which is an IBM 7300 digital magnetic tape unit. Separating the timing of the two processes was accomplished by adding a separate FET analog gate to each range circuit for readout. When a recording cycle starts, data is converted and recorded at the tape recording rate so that no buffer is needed.

The major differences between the WRSI and the IP are the bidirectional analog gates used in the IP as opposed to the unidirectional analog gates used in the WRSI, and the addition in the IP of a readout gate in each range block, allowing the complete separation of the acquisition and recording timing systems. The WRSI which uses bipolar transistors for the analog gates requires coincidence in the acquisition range timing and the current range block conversion, resulting in a slow down of data acquisition. The additional readout gates of the IP allow data conversion and recording regardless of the acquisition range

timing. The basic clock rate of the acquisition circuit is 186.2 KHz (0.5 statute miles), whereas the conversion-recording clock rate is 20 KHz, as required by the digital tape unit.

THE ILLINOIS PROCESSOR

Pages 5, 7, and 9 in the Appendix are block diagrams of the Illinois Processor, hereafter called the Processor. To test the Processor, a video square wave was used in place of the logarithmic receiver output. Photograph #1 in Figure 1 is the result of this test. Trace A is the simulated video input. Trace B is the integrated video input as viewed on the input video buss shown in Figure 1A on page 5 of the Appendix. The fifty range blocks were delayed to the center of the picture. Traces A and B are 0 to 2 volts and the square wave frequency is 10 KHz. Trace C is the video on the output buss of Figure 1A in the Appendix. The voltage is from 0 volts to about 2 volts and each of the fifty sampling periods is 50 microseconds long. The total sweep time is about 2.5 milliseconds. During operations this voltage is digitized and recorded. Traces A and B were synchronized with the transmitter pulse (PRF is 931 pulses per second), and trace C was synchronized with the recording cycle.

Photographs #2 and #3 (Fig. 1) illustrate tests of the integration process of the IP. Every 24 transmitter pulses a 2 V video pulse was applied to the input. The input was 0 V for the rest of the time. Photograph #2 is a picture of the 24 pulse cycles, and photograph #3 is a picture of the 2 V video pulse portion of that cycle. A similar test was used to obtain the measurements of the performance as described in paragraph 1 on page 12 of the Appendix. The integration process fulfills the design requirements.

The data recorded on digital tape by the Processor is the integrated video signal from a logarithmic receiver. Since it was difficult to match all the analog gates, a calibration scheme was adopted. To correct for the differences between range blocks, a calibration for each block was recorded and computer analyzed. The results were entered into the analysis programs for use as corrections. Corrections for range were also done by computer analysis rather than to use analog range correction. Also, the correction for measuring L_{avg} as an estimate of L_o was made during the computer analysis. Paul Smith (1964) describes the relationships and limits of intensity level and

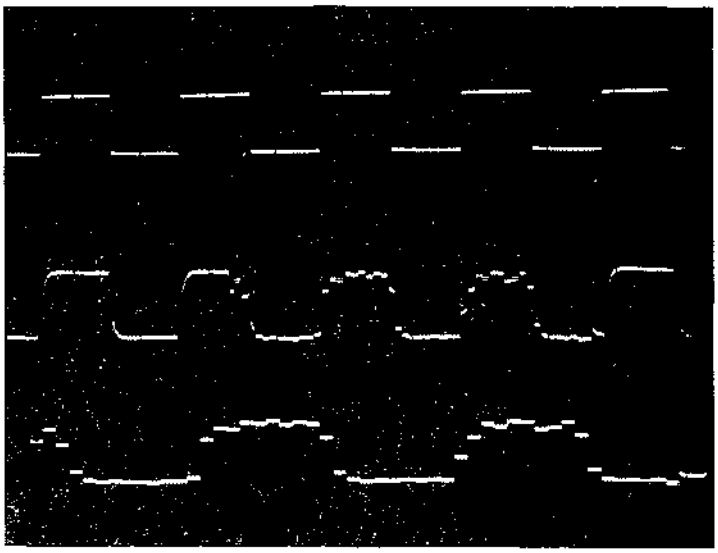

Photograph #1

	Trace	Function
A	A	Input video
B	B	Integrated input video
C	C	Output (sampled) video

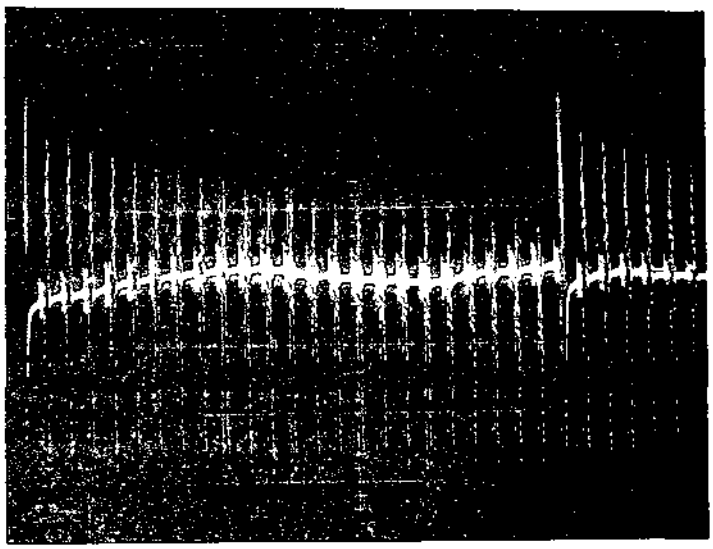

Photograph #2

Integration process left most

Photograph #2

Integration process: left most pulse is the 2 V video pulse applied to the 50 range blocks; the next 23 are the residual levels of the 50 range blocks on successive sweeps.

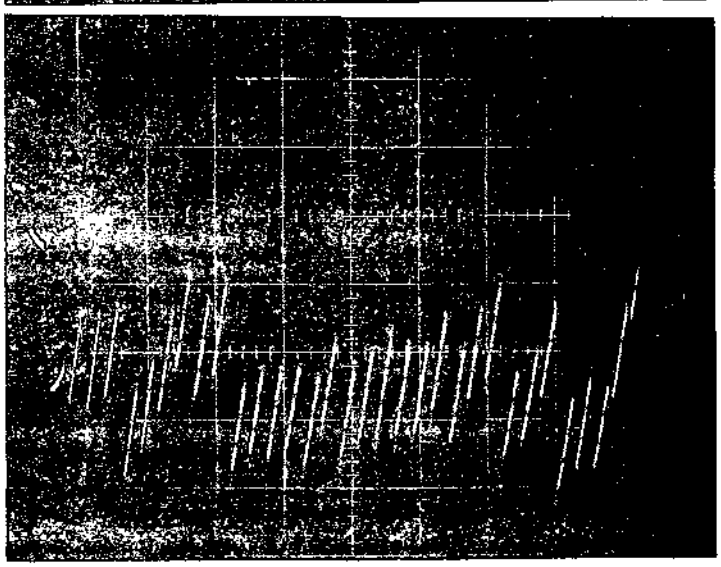

Photograph #3

Expanded view of the video pulse in photograph #2

Figure 1

the confidence limits of measured estimates of intensity level. The relation between Lavg and Lest is:

$$L_{avg} = L_{est} + .25$$

Since the Processor was intended for use as a research tool and not an operational tool, no real time data was generated.

Real time data displays could be generated with a little additional effort. The major difficulty in producing a quantitative real time display is the differences in calibration constants for the different gates. Either a more careful preselection of the gating transistors would be required or individual gain trimming potentiometers on each channel would be required. The latter method has been employed by the South Dakota School of Mines and Technology and by NSSL.

At present, the minimum time to produce quantitative data is dependent upon the available computer facility. At this university facility, results could be obtained between three and six hours after the digital tape was completed. The tape is not dismounted from the recorder until it is full, or the storm is over. When the Processor was first conceived, real time data was considered to be desirable but not essential.

When the Processor was being developed, a decision to use discrete circuitry was made on the basis of economy. Later this decision proved to be poor. The integration section was completed using discrete circuitry, and then the rest of the Processor was constructed from integrated circuit resistor transistor logic (RTL) and integrated circuit diode transistor logic (DTL). This latter section has proved much more reliable. The analog gates in the integration section required careful selection and handling. Some of the gates did not meet the requirements of the Processor even though they met the miminum manufacturer's specifications. Some of the gates were destroyed or degraded by handling, but this problem was solved after establishing careful handling procedures.

EQUIPMENT DELAYS

The first recording medium considered for the Processor was an eight-column paper tape punch which operated at 60 characters per second. This device would

have limited the Processor data collection rate to a slower rate than the theoretical rate for well-integrated data, but the paper tape punch was available. In May 1969, a surplus IBM 7300 digital magnetic tape unit became available. Incorporation of this device allowed the Processor to operate at its maximum rate, but required the redesign of the data conversion and recording circuits. These circuits were redesigned, and the radar interface and housekeeping data generators were designed and built. A digital clock that provided the day, hour, minute, and second also was completed. A ten-bit gray code azimuth angle encoder was installed in the radar pedestal. Since the first usage was to study surface rainfall rate-radar reflectivity relations, the radar was operated at zero degree elevation and no elevation encoder was necessary.

In the summer of 1969 the first of several long delays on delivery of components occurred. Integrated circuit plugs needed to complete the conversion, to magnetic tape were ordered in July 1969 but not received until February 1970. No vendor could provide better delivery dates than the selected vendor.

An order was placed with a business machine company in October 1969 for accessories and cables for the digital tape recorder. The local representative quoted a 90-day delivery time for the tape unit interconnection cables. At the end of May 1970, all accessories for the tape unit had been delivered, but the cables had not been delivered; furthermore, the local representative could not give a delivery date. The cable order was canceled and material was ordered to construct the interconnecting cables. This required using available connectors and partially rewiring the tape unit. The final cabling for the radar interface was delivered in April 1970. Since the last items completed were the tape unit cabling, the tape unit could not be tested until this was complete.

Contrary to its description in the surplus report, the tape unit was not operational when it was received. After the system was complete, tests on the tape unit revealed defective semiconductors, worn tape transport parts, and misaligned drive parts. After repairing and correcting some of the difficulties, an IBM serviceman was called to repair and adjust parts of the tape transport that required trained service personnel to complete.

After the tape unit was finally operating, the first attempts were made to collect data in August 1970. When the tapes of data were taken to the University computer facility, the tape format proved to be incompatible with the IBM computer system. It was then discovered that the format specified by available manuals was incomplete, and information obtained from the computer facility was

was in error. The correct information was obtained from an IBM engineer, and the recording circuitry was then changed to produce an IBM compatible recording format. After this problem was solved, data were successfully collected and read on the University computer system.

When data could finally be collected funds had been expended and operations were limited to September 1970 and data collection occurred on 3 storm systems. Two of the three storm systems did not pass over the operating part of the network. This left radar data on one storm system that could be compared with the network rainfall data.

DATA COLLECTION

Numerous unavoidable delays in the construction of the Processor, which are enumerated in an earlier section of this report, led to its completion at the time funds for this contract had been depleted. However, a data collection period in August-September 1970 was accomplished using support from other grants and the State of Illinois for the radar operations , raingage network operations , analyses of the data, and preparation of this report. This funding situation restricted the data collection period to 3 days in September 1970. Unfortunately, on only one day did convective storms occur over the 225-square-mile network during radar operations. These data are those analyzed and discussed in this report.

On September 3, 1970 a storm system crossed the raingage network. Data were collected on this system from 1250 hours to 1325 hours , by which time all radar echoes had moved over or disappeared from the 255-square-mile network. Part of the raingage network had been closed down, but this 255-square-mile portion of the network was kept operational to provide data for this research. The raingages were weighing bucket recording gages using 6-hour charts and 12-inch orifices.

Within the area of interest there were 25 raingages located in a 5 by 5 array with three miles between gages. Figure 2 is a drawing of the area of interest including the raingage network. For analysis the network was divided into 25 squares, 3-miles on a side. Each square was subdivided into 9 subsquares 1-mile on a side. The subsquares were numbered from 1 to 9 as shown in Figure 2, and the squares contain the gage number. Since the raingage network was set out on a statute mile grid before this investigation, the analysis of this work

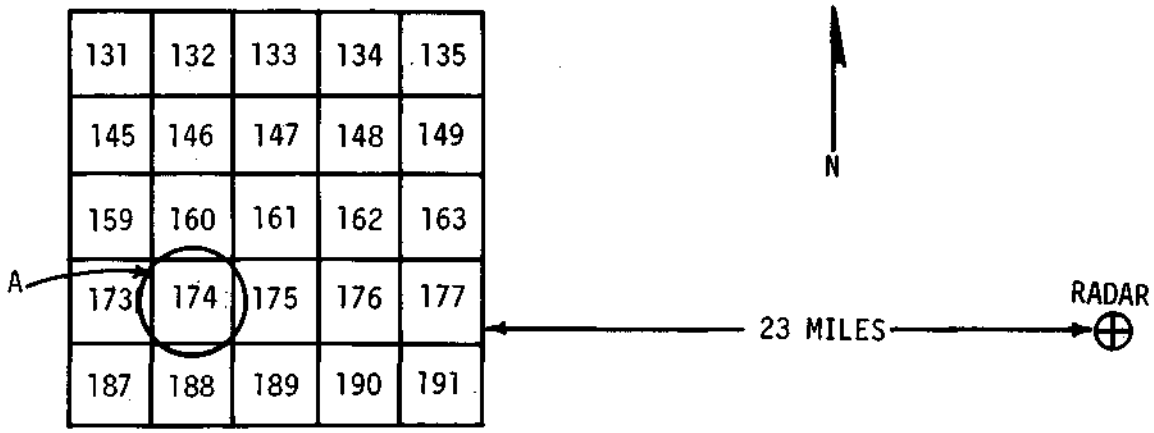

RADAR RAINGAGE NETWORK AND RADAR LOCATIONS

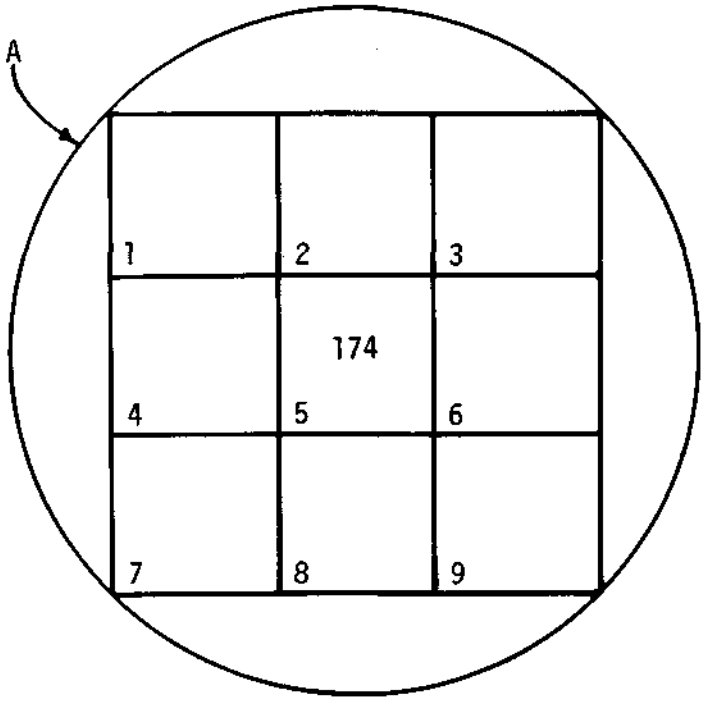

Figure 2. Raingage square and 9 sub-squares

was done using statute miles as a unit of measurement. The use of mile hereafter means statute mile.

The radar used in the investigation was a CPS-9/XE-2 weather radar. The CPS-9 is a 3 cm. radar that has an antenna beam width of 1 degree. Peak output power for short pulse operation was 135 KW. Short pulse (0.5 μs pulse length) was used throughout the investigation. The pulse repetition frequency was 931 pulses per second. The antenna elevation remained at 0.0 degrees for the entire investigation, but since no data from less than 24 miles was of interest, ground clutter was not a problem.

The Processor utilizes a logarithmic receiver from the WSR-57. The video output from this receiver is averaged by the integrator section of the Processor. The integrator section contains 50 identical analog circuits which represent 50 contiguous range blocks each of which is 0.5 mile long. The range chosen for the first block is selectable, in 8-mile increments, from 16 miles to 72 miles. The remaining range blocks are contiguous with each block 0.5 miles further in range than the preceding block.

A range block length of 0.5 mile provides poor resolution for observing convective rainfalls as shown by the results obtained. The l-degree beam width of the CPS-9 radar is. 0.4 mile wide at a range of 24 miles and 0.7 mile wide at a range of 42 miles. Thus, the range resolution is better than the azimuthal resolution for the majority of the area under investigation. Reducing the range block length would be beneficial if the beam-width of the radar. could be simultaneously narrowed, thus improving the aximuthal resolution; however, this is difficult and expensive.

The integration time of this Processor is fixed and the integration includes 30 separate transmitter pulses. Because time to independence of measurements of a volume in space is related to the shuffling rate within the volume, not all the pulses are independent. This turbulence or mixing is related to the radar Doppler spectrum, as noted by Lhermitte and Kessler (1965). For standard deviation of the Doppler spectrum of 0.7 m/sec, the time to independence is about 10 milliseconds. Therefore, in 30 transmitter pulses, about 3 pulses are independent. The time to independence would limit the antenna azimuth velocity to an unaccpetably slow rotation unless some range integration also occurs. In range the time to independence is half the transmitter pulse length. Since the CPS-9 pulse length is 0.5 micorseconds, and since the range block is about 5 microseconds long, each transmitter pulse produces 20 independent samples in each range block. Unless the rain is homogenous throughout the range block,

the samples are taken from separate populations and the result is in error. Since raingage data show correlations of +0.85 between points separated by 0.5 mile, the error normally should not be severe. Combining the effects of range and time integration, the measurement of L_{avg} includes a minimum of 60 independen samples. This measurement, plus correction for averaging the logarithm of intensity, yields a value for L_{est} within ± 2db of L_o at the 95% confidence level. This analog estimate of L_o is then digitized and recorded, along with the housekeeping date, on IBM compatible digital magnetic tape.

Radar data consisting of photographs of the PPI using gain-stepped video were collected simultaneously with the processor operation. These data were used to calculate total water accumulation and average rainfall rate over the network, and to draw echo shapes for comparison with Processor data.

ANALYTICAL TECHNIQUES

Three forms of data were available. The digital data on magnetic tape, which was produced by the Processor, was in a suitable form for computer analysis. The radar film data required more manual handling since a film scanner was not available. This film was developed, and then it was used to trace echo outlines of the gain-stepped video. The tracings in turn were used for numerical calculations and to compare echo characteristics, using unprocessed video, with those observed using reconstructions produced from Processor data. The raingage data was also in a form not easily adaptable for numerical calculation. These data, which consist of continuous data on 6-hour raingage charts, were digitized and recorded on punched cards using an Auto-trol 4300 digitizer to perform the data conversion and recording. After these preliminary steps, all three forms of data were in a standard IBM compatible form, either punched cards or digital magnetic tape.

The first use of the Processor digital tape was to produce maps of the echoes. The data were placed on the Processor tape in a manner such that each record contained 54 characters of data. Fifty characters of these data were measurements of the returned power (P_r) from each of the fifty 0.5-mile range blocks. Another character was used to indicate the azimuth at which the power measurements were taken. Other data included the date, time, and range at which the first measurement was taken. These data were listed so as to produce a digital map similar to a radar type range-azimuth scan (B-scan). Figures 3, 4, and 5 are samples of these listings. For example, the first line of the listing (Fig. 3) contains information about the date (day number 246), the time

DAY	HR	MIN	OS	INC
246	12	50	1	3

AZIMUTH	SEC	RECEIVED POWER
246.80	32	1
248.20	32	1
249.61	32	22
251.02	32	1464
252.42	32	116983 1
253.83	32	31 1 11447962 1
255.23	32	2451 5169BBA51
256.64	32	1 3523878D8841
258.05	32	2223565789753
259.45	32	122 124536982
260.86	32	2 11111111 5
262.27	33	1111561
263.67	33	1147563
265.08	33	2233 16981 1
266.48	33	24761 231
267.89	33	2231
269.30	33	72 1
270.70	33	34
272.11	33	1
273.52	33	1
274.92	33	1 1151
276.33	33	1 123443
277.73	33	125A8631
279.14	33	125AB932
280.55	33	3 238999741
281.95	33	35899631
283.36	33	355442
284.77	33	12213211
286.17	33	1 211211 1
287.58	33	15111
288.98	33	1 1 2692 1
290.39	33	1 7AA91 2
291.80	33	2531 1 266 1
293.20	34	1 1 28A63
294.61	34	1 2366485
296.02	34	233 3
297.42	34	1 22
298.83	34	1
300.23	34	
301.64	34	
303.05	34	
304.45	34	2

Figure 3. B-Scan Listing of Processor Data

DAY	HR	MIN	OS	INC
246	12	50	1	3

AZIMUTH	SEC	RECEIVED POWER
246.80	44	1
248.20	44	1
249.61	44	22
251.02	44	1464
252.42	44	116962
253.83	44	31 112449952
255.23	44	242 6388AAA51
256.64	44	352599CC8841
258.05	44	1222345567A8741
259.45	44	121 125337A711
260.86	44	1 1211331 1
262.27	45	1 1111541
263.67	45	147663
265.08	45	2222 26961 1 1
266.48	45	2674 21 1 1 1
267.89	45	2231
269.30	45	261
270.70	45	64
272.11	45	11
273.52	45	1 1 1 1
274.92	45	131
276.33	45	233462
277.73	45	1 125A963
279.14	45	125AA932
280.55	45	3 1 268AA972
281.95	45	35799741
283.36	45	1 353542 1
284.77	45	122131
286.17	45	11211
287.58	45	1 13211
288.98	45	2691 1
290.39	45	1 7A9711
291.80	45	365211 4693
293.20	46	1 1111 49A631
294.61	46	1 46684
296.02	46	3333
297.42	46	1 5
298.83	46	1 1
300.23	46	1 1 2 1
301.64	46	1 2
303.05	46	5
304.45	46	3 1 1
305.86	46	1

Figure 4. B-Scan Listing of Processor Data

DAY	HR	MIN	OS	INC
246	12	52	1	3

AZIMUTH	SEC	RECEIVED POWER
246.80	44	1
248.20	44	
249.61	44	1 1
251.02	44	121 1
252.42	44	28541 1
253.85	44	1 25861
255.23	44	123 1 1 6648841
256.64	44	1352 767A9A852
258.05	44	233478889851
259.45	44	2 3444658644 1
260.86	44	1 12324794
262.27	45	1 112111 1
263.67	45	1 1 1145
265.08	45	2365871
266.48	45	21 27AA81
267.89	45	653 2774 1
269.30	45	2231 111
270.70	45	23 1
272.11	45	296 1
273.52	45	33 1
274.92	45	1
276.33	45	1 141
277.73	45	354242
279.14	45	17A9421 1
280.55	45	1 1398741
281.95	45	1358AA831
283.36	45	13799941
284.77	45	1 12535521
286.17	45	112221111 1
287.58	45	1 21121
288.98	45	23111
290.39	45	28611
291.80	45	1 3895 1
293.20	46	158511 863
294.61	46	2111 866
296.02	46	1 469A31
297.42	46	1 1 2 331
298.83	46	1 1
300.23	46	1
301.64	46	1
303.05	46	1
304.45	46	2 1
305.86	46	1

Figure 5. B-Scan Listing of Processor Data

(hour 12 and minute 50), the range of the first measurement (24 miles), and the range block size (0.5 mile). The AZIMUTH column is the antenna pointing position, while the SEC column is time information indicating the second during which the measurement was made. The numbers in the map are measurements of P_r. The left measurement is at a range of 24 miles, and each successive measurement is for each 0.5-mile further out in range. A dash indicates the average P_r was below the lowest conversion level. This level was set just above the noise level so the number 1 represents the minimum detectable signal, or sometimes noise. The numbers in the map progress from 1 through 9 and then from A through V representing 31 levels of P_r each progressively greater. The levels are 2.5 db apart resulting in a dynamic range of about 70 db (which is greater than the dynamic range of the receiver).

These listings were used to graphically reconstruct the echo shapes of the observed storms. Since each number in the map represents the average P from a range block, and since each range block was 0.5 mile in length and varied from 0.4 to 0.7 mile in width, the variations in P_r with position tend to be smoothed. These reconstructions are shown in the two bottom maps of Figures 5, 6, and 7. The 2 top maps of these 3 figures are tracings from the photographs of the gain-stepped PPI display. An attempt was made to draw the isoecho lines in the reconstructions for the same levels of P_r as shown from the film data, but because the Processor produces discreet data and each gate sensitivity is necessarily the same, the isoecho lines are only approximately equivalent.

These figures were used to calculate the velocities of the echos. The displacement of the centroid of each echo was measured at the 5-minute intervals represented in Figures 6, 7, and 8. The velocities of the echoes did not vary significantly over the 20-minute period, and both the Processor and film data yielded echo velocities of 35 miles per hour from an azimuth of 232 degrees for both echoes shown.

It can be readily noticed that the Processor smooths the echo edges significantly. The levels depicted are as nearly as possible to the same sensitivity level, but nonetheless, some differences may exist. At 1256 (Fig. 6) in the southeastern echo, a Y-shaped channel of no echo lies within the echo area on the photograph. This is not evident in the processed data. In both cases there are three inner contours or cores.

A valid question exists as to which of these depictions best represents the

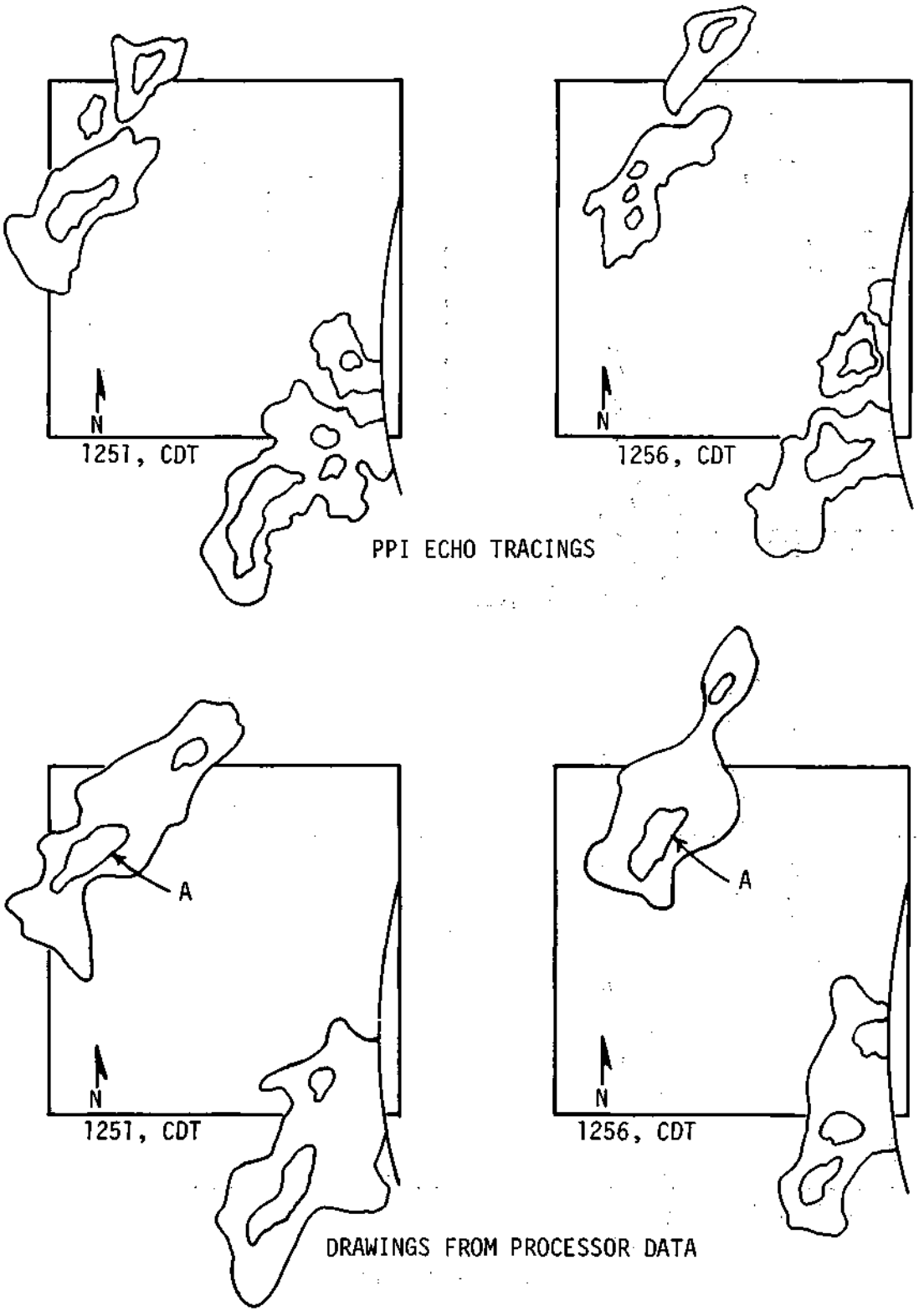

Figure 6. Comparison of Echo Shapes from Processor Data and PPI Photographs

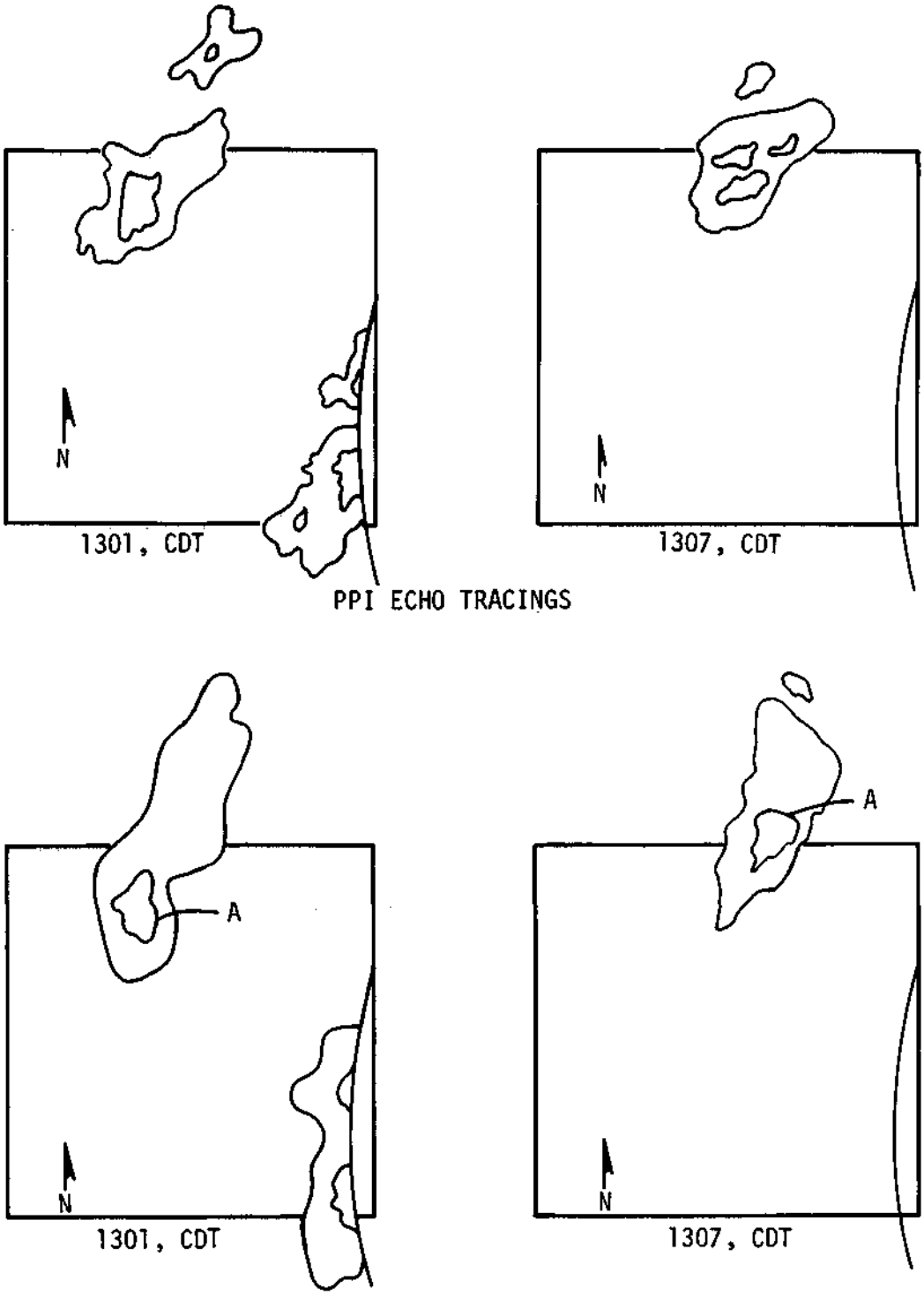

Figure 7. Comparison of Echo Shapes from Processor Data and PPI Photographs

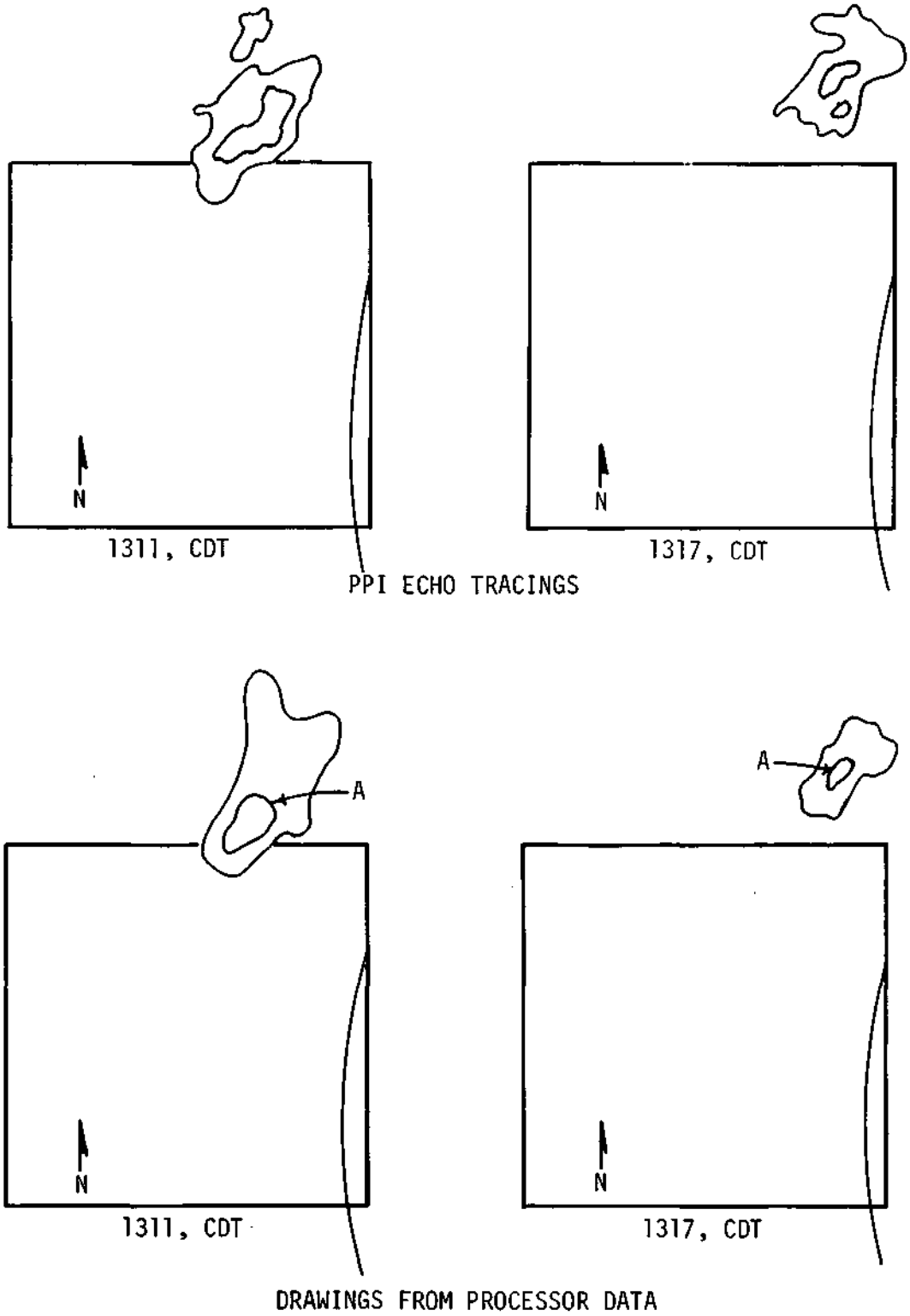

Figure 8. Comparison of Echo Shapes from Processor Data and PPI Photographs

natural rainfall patterns. The answer to this question cannot be derived from internal comparisons, and since both techniques possess so much greater resolution than the raingages, a comparison with the raingage data (gages spaced at 3-mile intervals) is without profit. One may argue that the lack of controlled integration in photographic recording produces erratic contouring just due to poor estimation of intensity. The apparent spatial continuity of the Y channel at 1301 suggests that this possibility is remote. Likewise the loss of range resolution by the integration technique may tend to cover such small perturbations in intensity. Again, this should not have happened on the upper portion of the Y which was essentially along a radial from the radar and should have been visible under range integration.

Although in all the calibration steps the Processor was 1 to 2 db more sensitive than the photographic recordings of the PPI display, the absences of the Y-shaped channel in the preprocessed data may or may not be due to sensitivity differences. Thus, one is left with the observation from limited data that one of the techniques is producing a poor estimate of the mean intensity. After more data are collected a definitive answer as to which is most valid should be determinable by comparison of patterns with raingage isohyets from a denser network. However, on the limited data available at this time, it is not possible to show which pattern and data are most appropriate. It is believed that the processor pattern will eventually be shown to be best.

TEMPORAL VARIABILITY OF REFLECTIVITY

One intense portion, or core, of the northwest storm (labled A on Figs. 6, 7, and 8) was followed for 6 minutes and 24 seconds of its lifetime using the B-scan listings. The reflectivity (Z) of the core was recorded and then graphed as a function of time (Z(t)), as shown in Fig. 9. Since the integration was performed over a block approximately 0.5 mile square, the Z values obtained are smaller than the peak values within the blocks. The values of Z were calculated from the measured P_r using the radar equation derived by Probert-Jones (1962)

$$P_r = \frac{P_t \pi^3}{2^{10} \ln 2} \frac{h}{\lambda^2} \frac{G^2 \theta_1 \Phi_1}{R^2} \left| \frac{m^2 - 1}{m^2 + 1} \right|^2 Z$$

As an illustration, the largest value of Z averaged over 1 square mile for 1 minute was 42.2 dbZ. The largest value of Z measured in any one range block during that time was 48.1 dbZ. The largest value of Z calculated from the raingage data taken near the same time was 49.4 dbZ. This value of Z was calculated from a 2-minute average rainfall rate at a raingage using the Mueller and Sims (1966) rainfall-reflectivity relationship for Illinois.

$$Z = 367 \ R^{1.41}$$

This single observation would support the contention that the basic block size of the Processor is a reasonable size with respect to a time resolution of about 2 minutes, for raingages. However, it should also be noted that using a single raingage measurement to represent an area as large as 9 square miles (the density of the network used in this study) is obviously inadequate if time resolutions as short as 2 minutes are applied to the data from raingages.

The data used to construct Fig.9 was also used to compare the projected location of a storm core, with the later location of the core. The velocity of the centroid was used as the storm velocity, and the position of the core at 1250 hours was taken as the starting point. For all data the maximum Z occurred within one range block or one beamwidth of the predicted location. Moreover, the difference between the predicted and actual locations did not increase with time although the comparison was made at 12 second intervals over a 10-minute period using the location of the core at 1250 hours to predict all later locations.

Thus, at least in these storms on 3 September 1970 the morphology of the echo remained reasonably stable for relatively long periods of time. This important finding, if supported by future data, permits utilization of the positions of the maximum Z block at various times for the calculation of total cell velocity. It is much easier to implement the velocity calculation on this basis rather than requiring that some other parameter such as the centroid of the echo to be calculated and motion of the centroid observed. In more complex situations the existence of 2 or more separated blocks with the same values of Z would require a more refined approach.

Fig. 9 also indicates the sharp gradients of Z to be expected in short periods of time. The largest gradient observed was 12 dbZ per minute, and the largest 2-minute average of the gradient was about 8 dbZ per minute. This

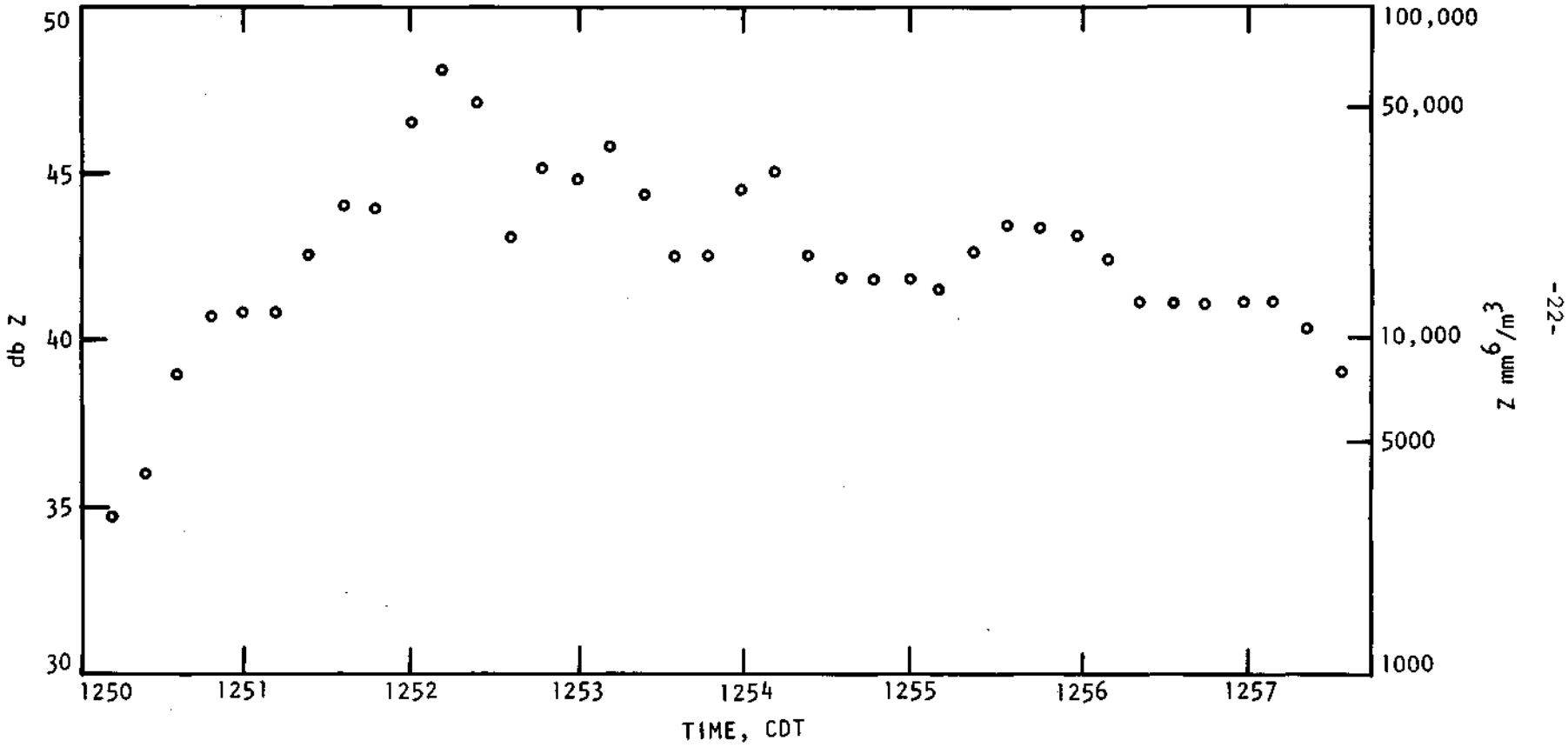

Figure 9. Cell Intensity Versus Time on September 3, 1970

data emphasizes the need for good time resolution when observing convective storms. Sampling times as short as 4 or 5 minutes may be inadequate.

Using the B-scan listing, the variation of Z with time in 4 contiguous ranges blocks at one azimuth was observed. The aximuth was 283 degrees. A graph of Z for the 4 range blocks is shown in Fig. 10. The northwest echo was moving 0.36 miles per minute across this azimuth and it was moving at 0.46 miles per minute toward the radar along the radial; these velocities were calculated from the average velocity of the echo centroid. The temporal gradient in a particular range block reach 18 dbZ per minute with a l-minute average of 12 dbZ per minute. The data used in Fig. 10 was chosen at a time when a core of the northwest echo was approaching and crossing the chosen azimuth. During the time the graph represents, the maximum Z of that core varied less than 3 dbZ.

In Fig. 11 the spatial gradient of Z is graphed for the difference of the four contiguous range blocks. The open symbols represent positive gradients, and the filled-in symbol represent negative gradients. Some 1-minute averages for the spatial gradients were 49 dbZ per mile, with values as large as 53 dbZ per mile. These values are conservative considering they were calculated from averages over an area about 0.5 mile square. The resolution of the Processor tends to smooth the data.

TEMPORAL AND SPATIAL RELATIONS OF ECHOES AND GAGE RAINFALL

Rainfall occurred at 7 of the 25 operational raingages on 3 September 19 70. To analyze the Processor data in the area of interest, a 21-mile square with the raingage network centered in it, was divided into a 21 by 21 array of 1 mile squares. Each raingage was centered in the 9-subsquare block, which puts the gage in subsquare number 5 (Figure 5).,

The P_r data on tape was converted to values of Z by the Probert-Jones radar equation (page 20). These values of Z were then converted to average rainfall for a range block by the Z-R relation for Illinois (page 21). For each subsquare the radar-indicated rainfall rate was obtained by averaging the calculated rainfall rate in all of the range blocks contained within each subsquare during each minute. These values were punched on to IBM cards. The total water accumulations for each storm and for the network were calculated at the same time from the average rate for each subsquare.

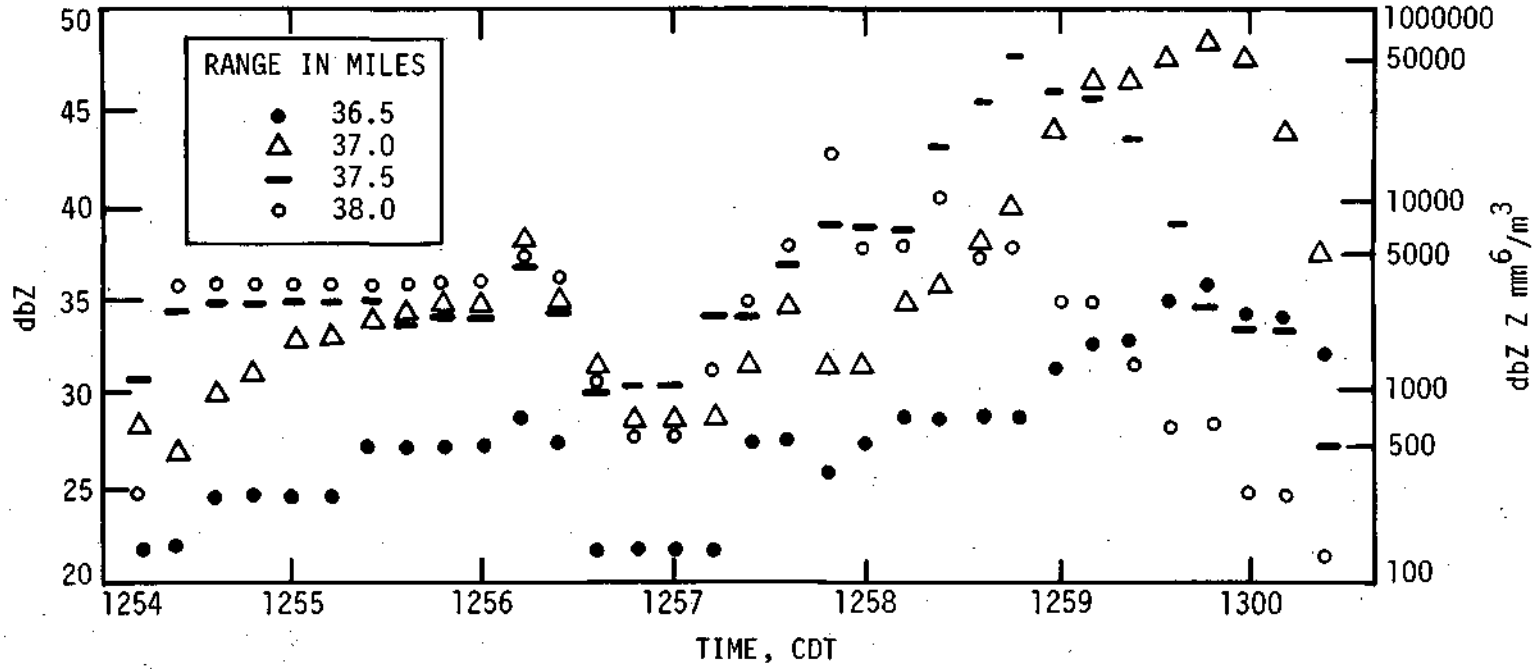

Figure 10. Reflectivity in 4 Contiguous Range Blocks on September 3, 1970

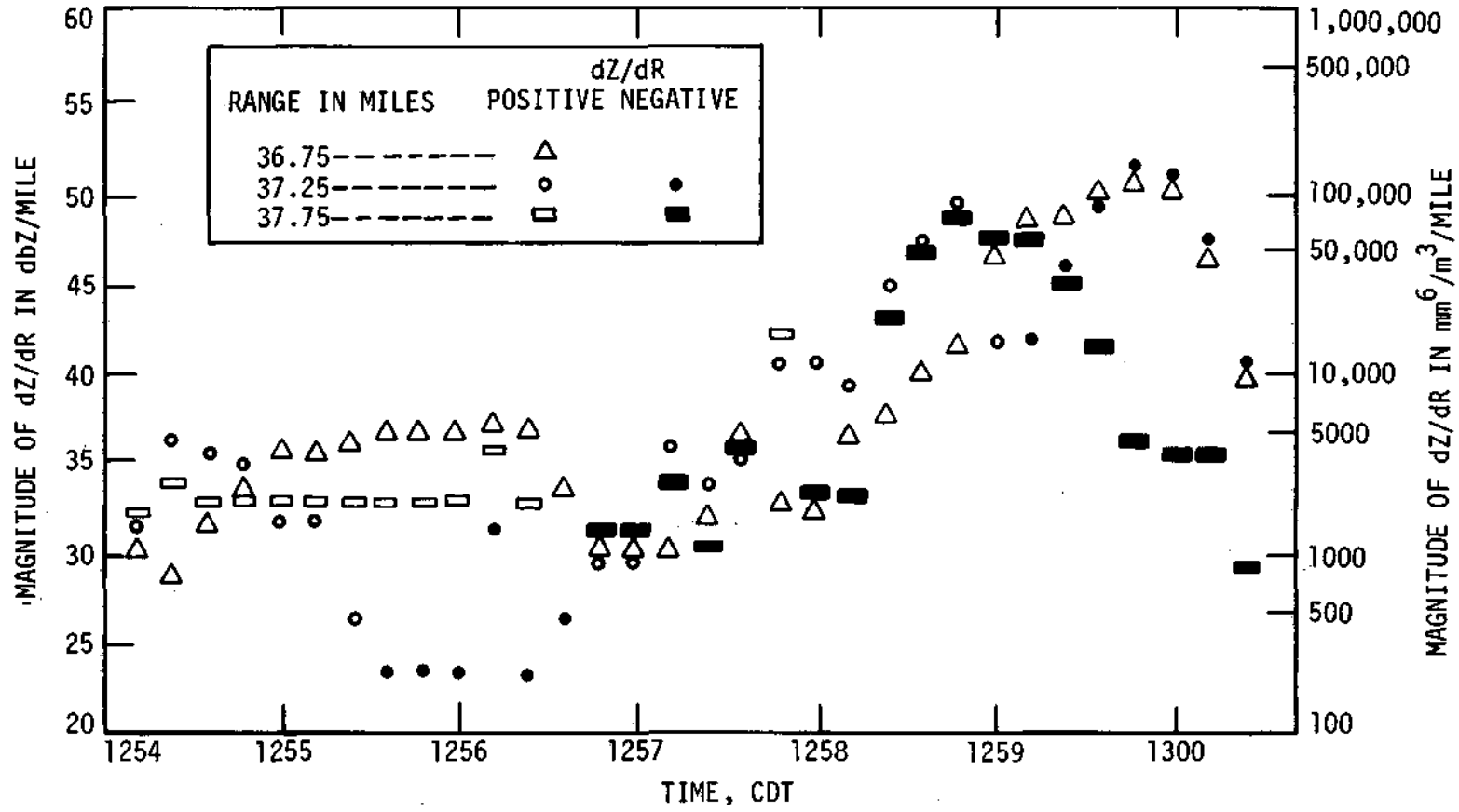

Figure 11. Reflectivity gradients Between Range Blocks on September 3, 1970

The rainfall rates punched on cards for each subsquare were then used to calculate time lag and spatial displacement correlations between the rainfall rates, as calculated from the Processor data, and those calculated from the raingage data. Errors in the raingage clocks, of ± 5 minutes, and the small displacements of the raingages from the centers of the blocks are problems that are difficult to treat in the analysis. The immediate effect of these "errors" would be to reduce the correlation coefficients calculated for this analysis.

Table 1 is a list of the correlation coefficients for time lags and spatial displacements for the two combined, storms data. Table 2 contains the same results for storm 1, and Table 3 is the same results for storm 2. In all but a few places in these three tables, time lagging the radar data with respect to the raingage data reduced the corrleation. It is possible that a time lag smaller than one minute would be beneficial.

Considering Table 1, the highest individual subsquare correlation is with subsquare 8, (south-central), although it is not markedly better than subsquare 7 (southwest). Thus, with no time lag the best correlation was obtained between the raingage and the subsquare centered 1 mile directly south of the raingage. The echoes had a component of motion toward the north but had a greater component toward the east.

The results of Table 3 for the southeast storm may be as one would expect. A high correlation was obtained for subsquare number 5 (over the raingage) with a 2-minute lag of the radar data. This 2-minute lag of the radar data would represent a drop fall of about 600 meters if an average fall speed of 5 meters per second is assumed. An equally high correlation is obtained with no time lag and subsquare number 8, and the highest was with subsquare 7 and time lag 4. The existence in both the combined as well as in the individual echos of high correlations with subsquare 8 is surprising. On the basis of this data no conclusion can be reached.

It is encouraging to note that when the entire 9-square-mile area is considered (Tables 1-3), the correlation is usually higher than for any one subsquare. This indicates some hope of obtaining good correlation with point measurements. The effect of increasing correlation with the large radar area may be physically explained in terms of the areal dispersion of the water between the beam measurement aloft and the ground, and the need for allowing for the differences in the resolutions of the two measurements. The raingage represents a specific point

Table 1. Correlation coefficients for combined storms with 81 (2-minute) samples from all 7 gages with rain

Sub-square	Time lag in minutes				
	0	1	2	3	4
1	.373	.307	.259	.212	.192
2	.316	.215	.241	.169	.184
3	.176	.096	.054	-.015	-.053
4	.399	.444	.258	.363	.207
5	.427	.207	.181	.106	.056
6	.104	.016	-.036	-.079	-.098
7	.523	.498	.365	.241	.170
8	.552	.345	.193	.119	.021
9	.228	.123	.279	.189	.098
9 mi^2 avg.	.561	.420	.279	.189	.098

Table 2. Correlation coefficients for storm 1 with 46 (2-minute) samples from 4 gages with rain

Sub-square	Time lag in minutes				
	0	1	2	3	4
1	.423	.332	.218	.145	.109
2	.324	.162	.163	.089	.111
3	.104	.022	-.035	-.076	-.019
4	.471	.491	.259	.339	.149
5	.445	.171	.114	.055	-.008
6	.076	-.021	-.061	-.110	-.107
7	.564	.532	.379	.232	.141
8	.560	.335	.170	.104	.008
9	.186	.065	.004	-.035	-.063
9 mi^2 avg.	.594	.423	.258	.159	.063

Table 3. Correlation coefficients for storm 2 with 35 (2-minute) samples from 3 gages with rain

Sub-square	Time lag in minutes				
	0	1	2	3	4
1	.142	.204	.423	.438	.532
2	.267	.501	.520	.610	.443
3	.619	.640	.585	.376	.240
4	.051	.200	.244	.518	.474
5	.382	.658	.704	.641	.531
6	.290	.189	.060	.018	-.125
7	.488	.655	.522	.699	.164
8	.704	.479	.432	.218	.113
9	.569	.513	.108	.052	-.102
9 mi^2 avg.	.638	.672	.639	.552	.488

measurement with relatively poor time resolution (2-minute) compared to radar sampling. The processed radar data on the other hand represent reasonably high time resolution but poor spatial resolution. Apparently better correlations can be obtained when the larger areas are used with the radar data because of a tendency to reduce the range of the variable by the preliminary averaging. In none of these cases can the 3-cm attenuation be responsible for the poor correlations since there were no intervening storms.

Figure 12 is graphs of the measured and calculated rainfall over the raingage networks. The first graph is for the northwest storm, the second graph is for the southeast storm, and the third graph is for the storm system. It is difficult to draw conclusions from the small amount of data used 'to construct the graphs, but the processor data seems to show a better temporal agreement with the raingage data than the film data does.

CONCLUSIONS AND RECOMMENDATIONS

The data Processor was made to operate in the manner in which it was designed. The amount of data obtained is woefully inadequate to permit the types of analysis required to properly assess the usefulness and accuracy of the Processor. Though the amount of data is limited, the accuracy of the Processor appears to be higher than the earlier stepped-gain method. Importantly, the analysis time is reduced significantly.

Possibly, the most significant meteorological implication of this work is the observation that the point of highest reflectivity traveled at the same velocity as the echo itself. Thus, if this result is supported by more observations , the velocity of an echo could be determined by determining the velocity of the highest reflectivity point. This is a much simpler task and one that can be easily performed automatically.

It is unfortunate that a large portion of time and resources of this contract had to be expended in developing a useful data Processor. Such a Processor is considered mandatory for any future research in quantitative radar meteorology. It is believed that the research initiated by this contract should be continued. The Illinois State Water Survey and the University of Illinois desire to continue this form of research and if permitted to do so, will collect more data in the coming seasons. An opportunity to pursue this appears to exist in 1971 rain studies of the ISWS. If so, the results of the analyses of these data will be furnished to the Atmospheric Science Laboratories of the U. S. Army.

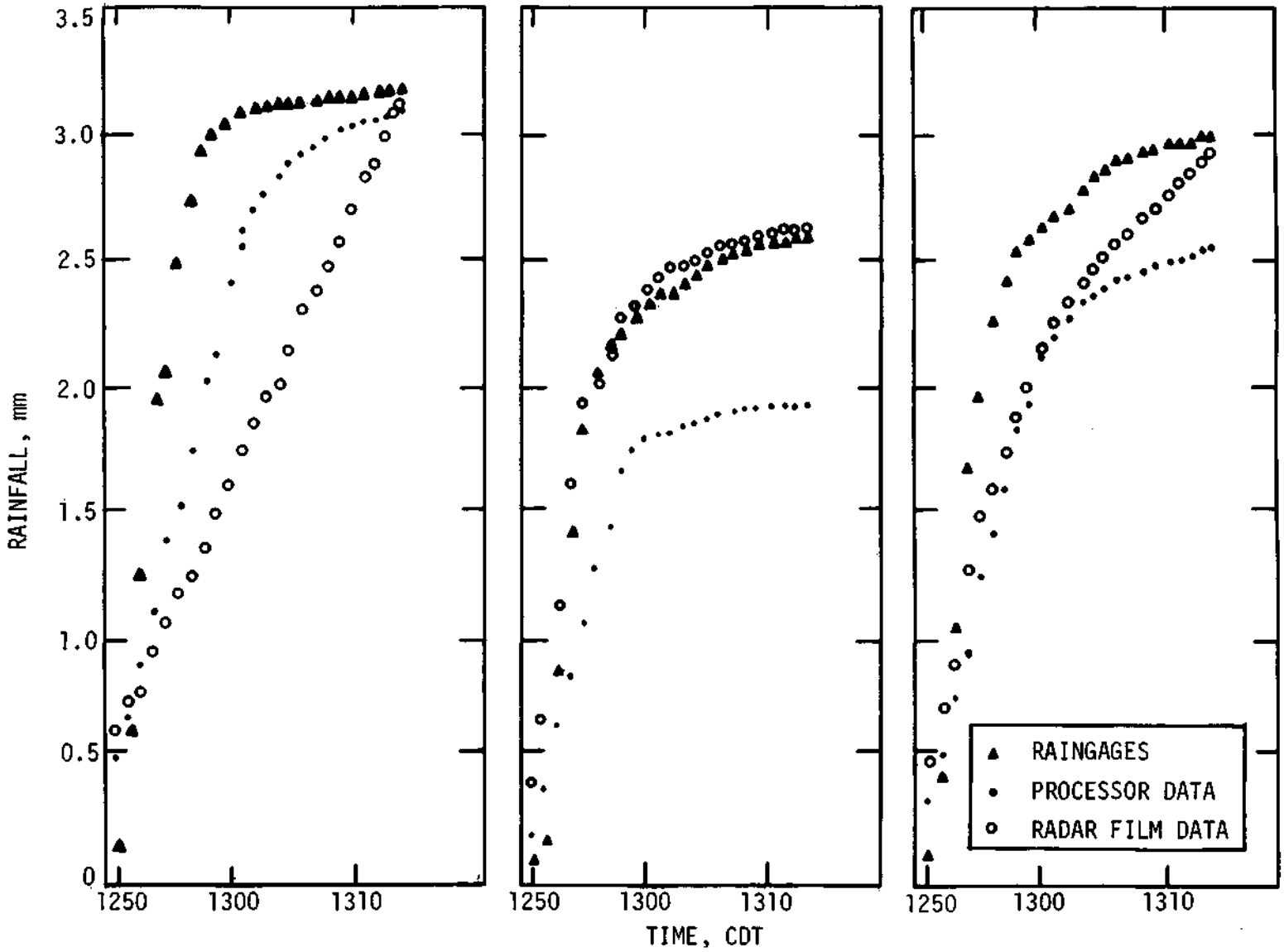

Figure 12. Calculate and measured rainfall

REFERENCES

Austin, Pauline M. , 1963: Application of Weather Radar to Fallout Prediction, Report DA 36-039 SC-75030, MIT, Cambridge, Mass.

Austin, Pauline M., 1969: Application of Radar to Measurement of Surface Precipitation, Research Report ECOM-0319F, MIT, Cambridge, Mass.

Farnsworth, G. W. and E. A. Mueller, 1956: The Theory and Operations of the Area Integrator, Research Report No. 5, Urbana, Illinois.

Jones, D. M. A., R. E. Rinehart, E. A. Mueller, D. W. Staggs, 1967: Evaluation of the Maser-equipped Radar Set AN/MPS-34 and Area Precipitation Measurement Indicator, Technical Report EC0M-01257-F, Urbana, Illinois.

Lhermitte, Roger M. and Edwin Kessler, 1965: Weather Radar Signal Integrator, Technical Memorandum No. 2, National Severe Storms Laboratory, Norman, Oklahoma.

Mueller, E. A. and A. L. Sims, 1966: Investigation of the Quantitative Determination of Point and Areal Precipitation by Radar Echo Measurements, Technical Report EC0M-00032-F, Urbana, Illinois

Mueller, E. A. and A. L. Sims, 1969: Relationships Between Reflectivity, Attenuation, and Rainfall Rate Derived from Drop Size Spectra, Technical Report ECOM-02071-F, Urbana, Illinois.

Probert-Jones, J. R. , 1962: The Radar Equation in Meteorology, Quarterly Journal of the Royal Meteorological Society, pp. 485-495, 1962.

Smith, Paul L. , Jr., 1964: Interpretation of the Flucating Echo from Randomly Distributed Scatterers: Part 3, Report MW-39, Scientific Report No. 1, AFCRL Contract No. AF 19 (628)-2489, Stormy Weather Group, McGill University, Montreal, Canada.

APPENDIX

PREPROCESSING AND RECORDING METEORLOGIC RADAR VIDEO

BY

EDWARD J. SILHA, JR.
B.S., University of Illinois, 1967

THESIS

Submitted in partial fulfillment of the requirements
for the degree of
Master of Science in Electrical Engineering
in the Graduate College of the
University of Illinois at Urbana-Champaign 1970

Urbana, Illinois

ACKNOWLEDGMENT

The author wishes to express his deep appreciation to his thesis advisor, Dr. Gilbert Fett, for his advice, and to Dr. Eugene Mueller, through whose direction and consultation this work was accomplished.

He would also like to thank the United States Array. Their interest in the work and funding made the project size possible.

Last, he would like to thank his family for the support and patience they continually provided.

PREFA

The objective ?? his thesis was to?? sign, build, and operate a data processing and ??ection system for use with a weather radar. A primary character?? of the system is that it has 'the flexibility to be used on any weather radar without impairing the normal operation of the radar for other purposes. Although it was tested on a CPS-9 radar, it is capable of being' u?? with most other scanning weather radars.

The processor requires a trigger coincident with the transmitter pulse, digital azimuth and elevation data, and a 30 MHz intermediate frequency (IF) signal from the radar. The 30 MHz IF must come from a preamplifier or from one of the first IF stages before any manual or automatic gain control can affect it and before the stages that will saturate on large signals.

The processor records data on digital magnetic tape that is compatible with the computing system at the University of Illinois. The recording device is an IBM 7330 magnetic tape unit, which is considered a part of the processor.

TABLE OF CONTENTS

1. INTRODUCTION

1.1 Choosing the system type.

Radar is a useful tool for weather observation. It allows the observer to remain in one location and monitor meteorlogic occurrences at ranges of 100 miles or more. More quantitative observations require some method of recording the data that the radar produces.

For years radar data has been recorded by photographing the Plan Position Indicator (PPI). This method has some serious defects. Film data must be analyzed by people, although some attempts have been made to use scanning devices to convert film data into a form easily entered into a computer. Man-months of effort have been spent analyzing individual storms that have life times of tens of minutes. Also cathode ray tube (CRT) phosphors have a dynamic range of about seven decibels (db) compared with a 60 db range encountered in weather echoes.' Controlling the total transfer function (including receiver gain, CRT intensity, film sensitivity, and film development) is difficult. This type of recording is only accurate to ± 5 db. [1]

The other means of recording weather radar data are using pure digital systems or using hybrid digital systems. Data rates for radars are high in the MHz region. Recording or processing digital data directly from the radar requires very fast equipment or large amounts of storage. A hybrid system offers the alternative of analogue circuits to preprocess the data and slow the rate before it is recorded in easy to use digital form.

The need for preprocessing the radar data before recording is due to the statistical variation in weather echoes, as outlined in the next section. This need is as great as the need for recording the data in an easily usable form, since recording the data is useless unless it has some true relation to the variables being measured.

1.2 Statistical considerations of weather echoes.

The amplitude (A) of the return from a weather echo is a superposition of many phasors, each of which is produced by a rain drop, hail stone, or snow flake.[2] The instantaneous signal return originates in a volume that has a depth equal to one half the length of the transmitter pulse (h/2). In this volume the weather target is composed of numerous small, randomly distributed targets that are continually reshuffling with respect to each other. This causes the instantaneous amplitude to vary randomly. The target intensity (I) which is proportional to A^2 will also vary as will the intensity level (L) which is proportional to the logarithm of I. The probability distributions for these variables are known with respect to their true value.[3] In relation to the true value of variable, the variance caused by the reshuffling of the random scatterers is equivalent to noise riding on the signal of interest.

Since weather echoes have a 60 db range, a logarithmic receiver is a logical choice to compress the range. An averaging process to reduce the echo variance will produce an average of the receiver output (an average of intensity level, L_{avg}). As the number of independent samples used in the average increases, the intensity level (L) approaches

an average intensity level (L_{avg}) which is related to the true intensity level (L_o) by the equation:[3]

$$L_{avg} = L_o - 2.5 \text{ db}$$

To get a good estimate of L_o a number of independent samples must be included in L_{avg}. Fifty independent samples would result in 95% confidence limits of ± 2 db. One hundred independent samples would result in 95% confidence limits of ± 1 db.[3]

Because the transmitter pulse illuminates a volume with a depth of the pulse length (h) over 2 (volume depth = h/2), each increment in range of h/2 provides a new set of scatterers, hence an independent sample. When a volume has been sampled, that volume does not provide another independent sample until the scatterers have reshuffled. This time to independence is inversely proportional to the wavelength (λ) since a scatterer must move a longer distance to change its phase relationship at longer wavelengths. Reshuffling takes place on the order of every 5 to 100 milliseconds depending upon wavelength and turbulence in the target volume. If the volume of interest is broken up into small blocks, the time to get an estimate of L_o for each block depends on the block size, wavelength, and target reshuffling rate.

1.3 Preprocessor.

The minimum block size chosen for this system was. a volume defined by the antenna beam width and having a depth of . 5 mile. The processor has 50 contiguous blocks composed of a memory capacitor

(.025 micro farads), an acquisition gate and a recording gate (Figure 1B). Figure 1A shows the interconnections of the 50 blocks. The switching ??ments are RCA 3N138 MOSFET's (Metal Oxide Semiconductor Field Effect Transistors). The input switch allows the capacitor to charge or discharge through the 5. GK timing resistor during the proper range period. This produces an exponential average with a time constant of 140 microseconds. Since the switches are only active during a particular range period which is about 5 microseconds (.5 statute miles), the capacitor charge represents samples from the last 28 transmitter pulses. A 5 microsecond block contains 10 independent samples when the transmitter pulse length is . 5 microseconds, as with the CPS-9 radar to which the processor is now attached. Therefore the capacitor charge represents about 280 samples, of which about 35 are independent samples.

The MOSFET's are effective analogue switches. The channel resistance with the gate to substrate voltage (V_{gss}) at + 2 volts is about 200 ohms. With V_{gss}) at -5 volts the channel resistance is on the order of 10^{10} ohms. These values were obtained in tests performed with 10 different transistors, and the results agree with the manufacturers specifications.[4] The MOSFET's are bidirectional (symetrical) gates so the memory capacitor can charge or discharge depending upon the input voltage. Discrete logic was used in the processing section because of the control voltages required by the MOSFET's.

With the processing section so determined, the peripheral circuitry design was straight forward.

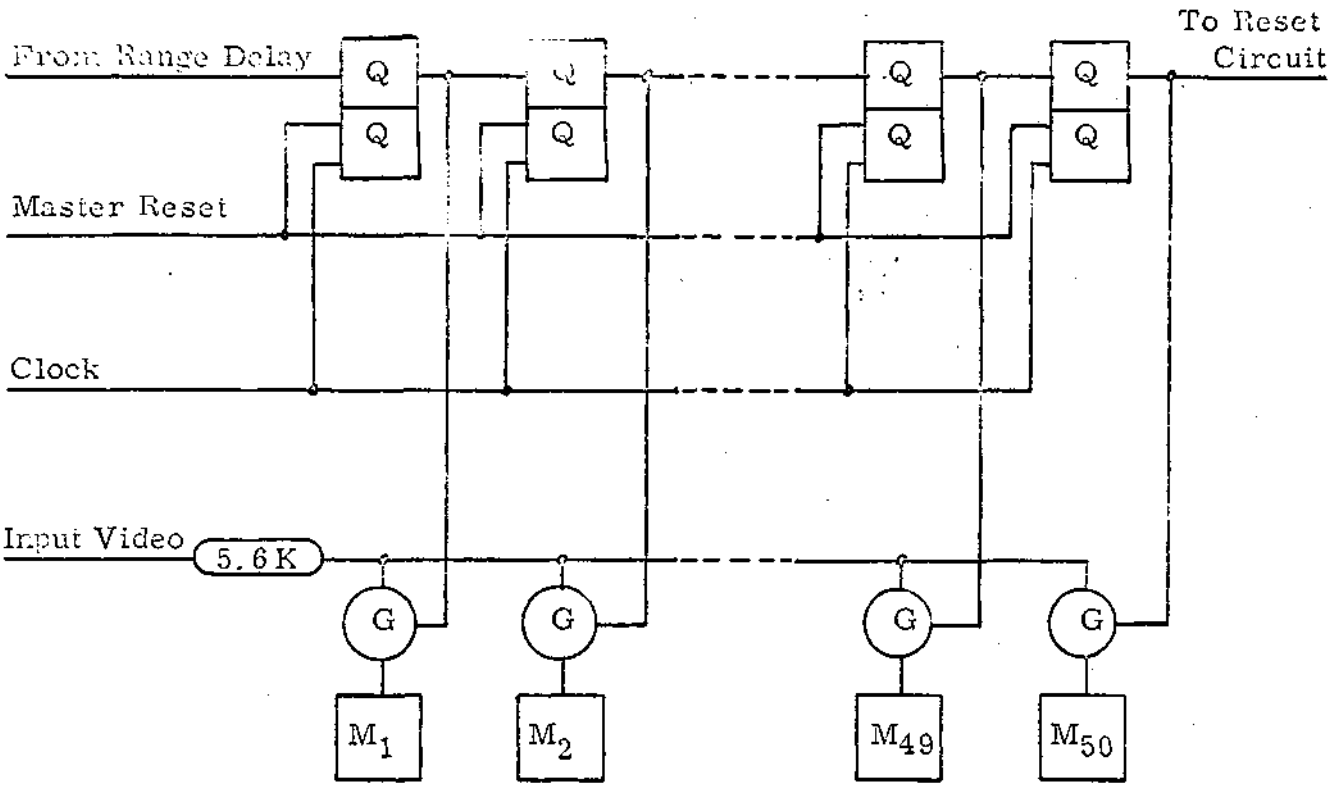

Figure 1A Block Diagram of Acquisition Shift Register and Memory Elements

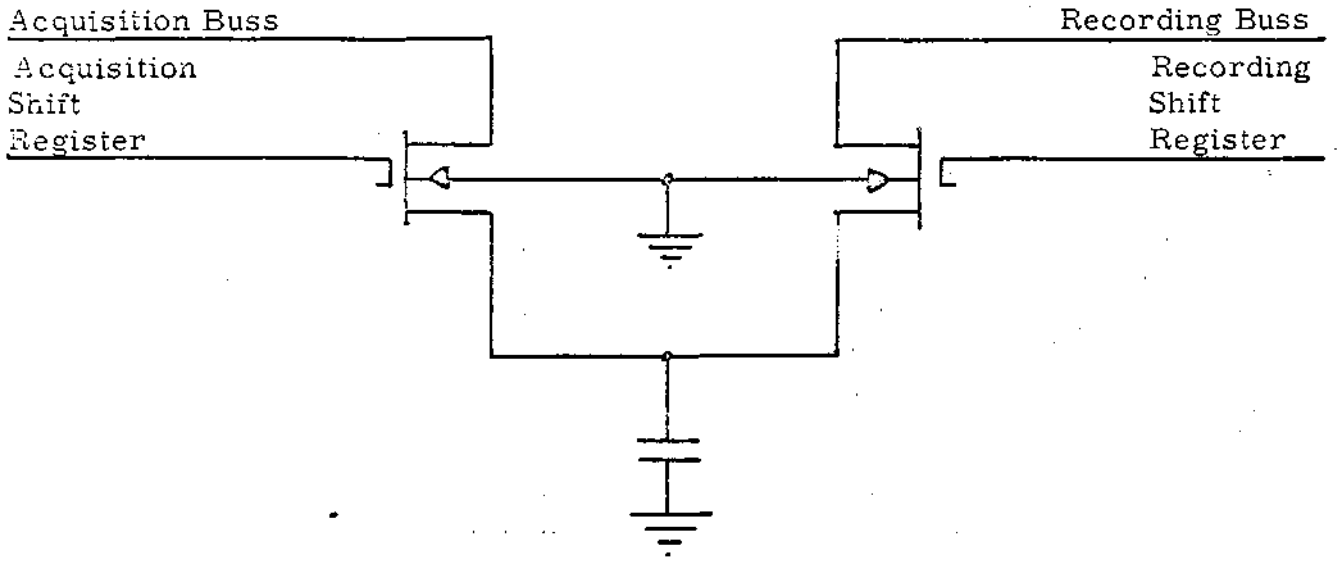

Figure 1B MOSFET Gates and Memory .

2. THE SYSTEM FORM

2.1 Acquisition timing.

The processor has two timing systems, one for data acquisition, and another for data recording. This feature was built in to allow the processor to operate with different radar sets and different recording devices. The seperate timing of the acquisition and the recording sections is a necessary requirement for the system. Any weather radar data processor must have the acquisition timing controlled by the radar pulse repetition frequency (PRF) and the velocity of propagation of the transmitted energy through free space. The recording section timing is fixed by the recording device characteristics. Attempts to interleave or synchronize the two timing controls severely restricts the processor flexibility. The seperate timing is made possible by using seperate switching transistors for acquisition and for recording.

The acquisition timing system requires a trigger from the radar to establish a reference time (Figure 2). The trigger gates a 1.4896 MHz oscillator to a 4 bit counter. The output of the counter provides . 5 statute mile pulses. The pulses are counted down to an operator selected delay of from 16 miles to 7 2 miles in 8 mile steps. After the delay time has expired the . 5 mile pulses are counted in the gate length circuit. The output, which is operator selectable at .5 mile, 1.0 mile, or 2. 0 miles, drives the acquisition shift register clock line. This causes the one bit loaded in the gate, G1, by the range delay circuit to be shifted through the register enabling one memory element at a time. When the bit is shifted

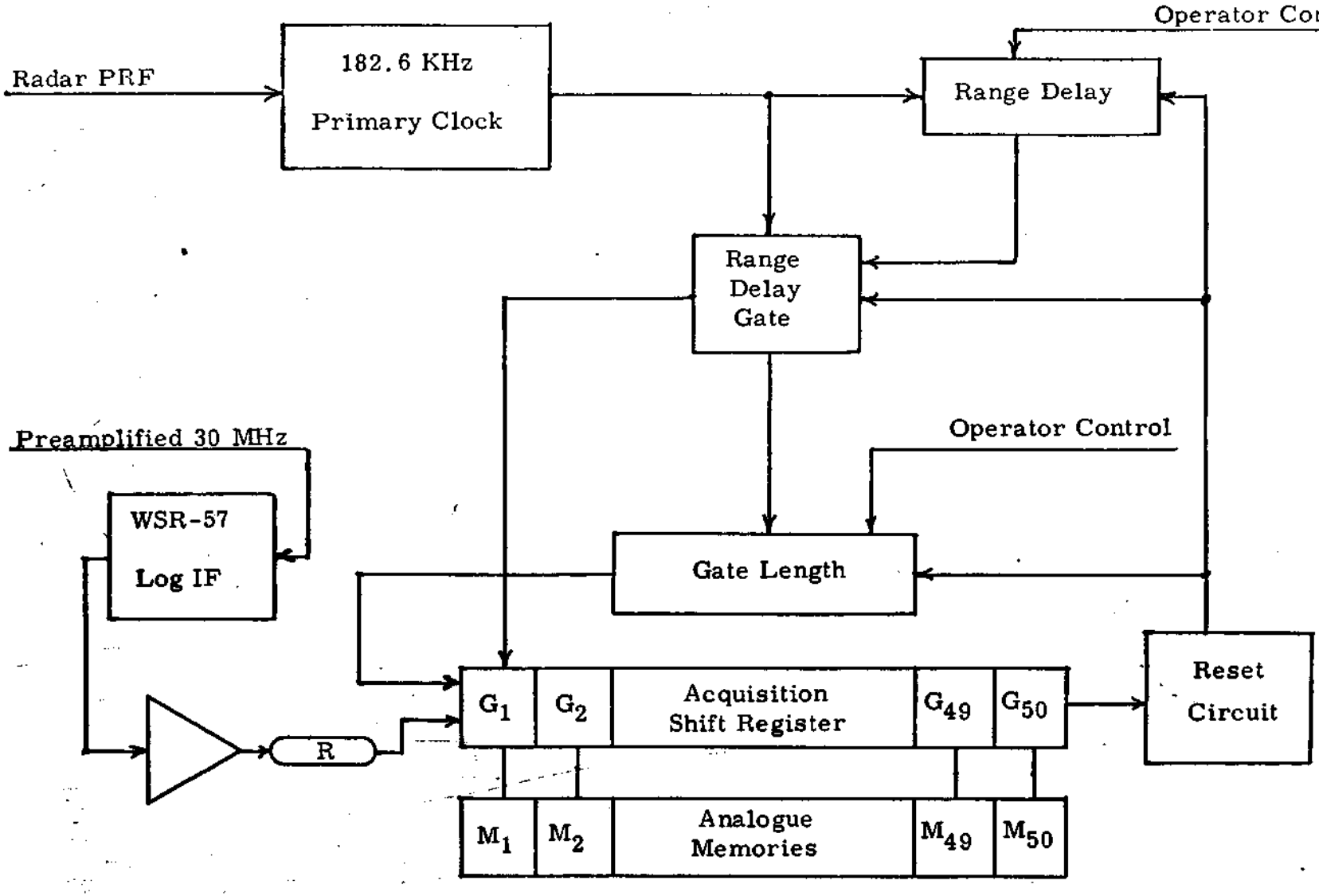

Figure 2 Acquisition Block Diagram

out of G50, it resets the acquisition timing circuits, readying them for the next acquisition cycle.

2.2 Recording timing.

The recording shift register is identical to' the acquisition shift register except the clock line is driven by the clock that controls the IBM 7330 magnetic tape unit. The analogue switches are connected to the same capacitors as those in the acquisition circuit, but the recording bus line terminates in a high impedance amplifier so that sampling the block does not drastically change its state of charge (Figure 3). The output of the amplifier is fed to a 5 bit 30 KHz analogue to digital converter (A/D) which produces the numbers 0 to 31 for voltages of 0 volts to 2 volts. Since the logarithmic receiver has a 60 db range, the output numbers represent about 2 db steps.

The tape control also samples the housekeeping data each time it writes a record. A record contains 65 characters. The first fifteen characters are housekeeping data, and the rest are block values, one for each range block. Antenna azimuth data is provided by a digital optical encoder. This data is in gray code form to reduce the ambiguities produced by standard binary when bits change during the sampling period. A digital clock, part of the processor, provides the day of the year, hours, minutes, and seconds to a buffer. Range delay and gate length data are taken from the operator controlled switches. Elevation data is not available on the CPS-9 radar, but the processor has the circuits for recording elevation if or when it becomes available.

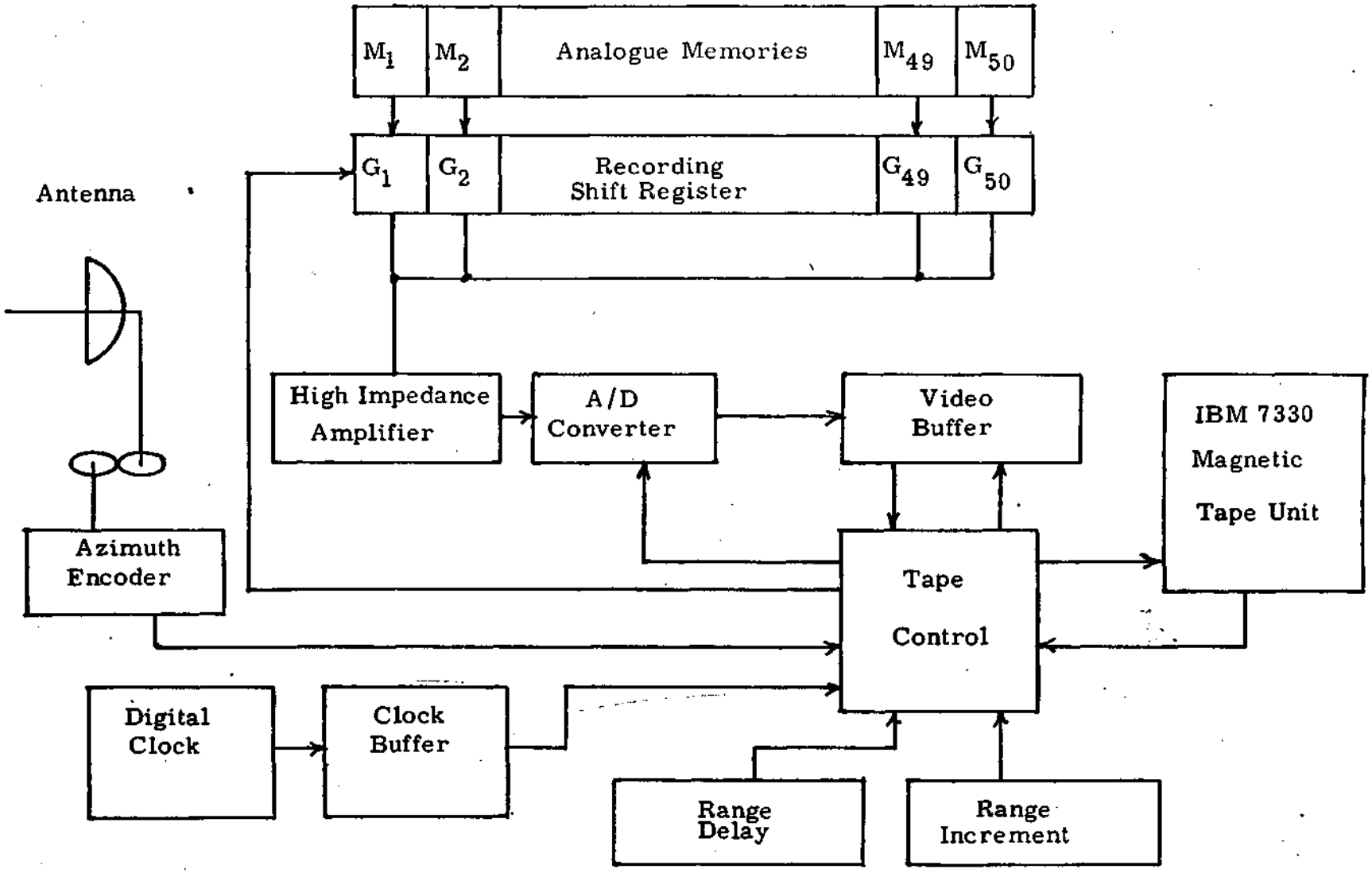

Figure 3 Recording Block Diagram

3. SYSTEM TO RADAR INTERFACE

3.1 Trigger.

The system to radar interface is relatively simple. The trigger pulse taken from the radar must be changed to the proper level and polarity. The CPS-9 radar produces a 30 volt to 60 volt positive pulse with noise voltages up to 10 volts in amplitude. An inverter circuit with a 20 volt threshold is used to produce the negative 12 volt pulse required to start the acquisition cycle.

3. 2 Azimuth data.

Azimuth data was obtained by installing a Baldwin 10 track optical encoder in the antenna azimuth drive linkage. The 10 bit gray code output from the encoder is brought from the antenna to the processor through Belden 9 pair, foil shielded cable. The azimuth data inputs drive level translators to produce logic levels compatible with the Motorola MDTL logic that was used to build the recording control section.

3.3 30 MHz IF

A 3N138 MOSFET is used as the input stage of the 30 MHz IF line driver. The input to the line driver is taken from the grid of the second IF stage of the CPS-9 radar receiver. Since the CPS-9 has only one video slip ring in the pedestal, the output of the 30 MHz IF line driver is mixed with the video signal and brought from the antenna to the processor on the normal video transmission line. At the radar console the video and IF are seperated with the video resuming its normal course,

and the IF signal being brought to the logarithmic IF strip in the processor. This IF strip is from a WSR-57 weather radar, with power supplied by a transistorized power supply. The IF strip is a tube type amplifier.

4. SYSTEM PERFORMANCE

The exponential averaging performed by the preprocessing section is adequate. The time constant was measured by applying one video pulse for every 30 cycles of the processor. On the 30th cycle the voltage had dropped to 32% of its initial value as opposed to the 34. 2% calculate from the RC combination. There was no difference between the calculated and measured values of the charging time constant.

Some problems occurred because the blocks were not quite identical. This is due in large part to the leakage current in the source to substrate diode of the MOSFET's. There are two solutions to the problem. One is to select the 3N138 MOSFET, which is expensive, time consuming, and not very rewarding. The other solution is to calibrate the gates and perform a linear regression analysis on each gate, then use the numbers in the analysis programs to get corrected values. This solution is very convenient. A calibration tape is recorded. The input values are entered into a computer program which reads the tape, does the regression analysis, and punches a deck of cards, which are used by the data analysis programs to normalize the data. The results of a calibration are listed in the Appendix.

There appears to be a lot of switching transients on the video lines. A solution to the problem may be to roll off the switching waveform edges.[5]

At present the AC power to the processor is furnished from the radar modulator. This power line is noisy and when the radar mode is

switched from one pulse length to another or when the transmitter is turned on or off the tape unit sometimes malfunctions. This problem can be corrected by obtaining power from a different line or by getting it near the main power transformer.

5. CONCLUSIONS

The MOSFET switch allows the acquisition timing to be seperated from the recording timing. The recording section functions seperately from the acquisition section, with the processing section acting as a buffer between the two sections, although its primary purpose is averaging the echo intensity levels.

It proved difficult to match the range blocks due to variations in the MOSFET's. The primary cause of this problem is the leakage current in the source to substrate diode in the MOSFET. Since matching the blocks proved difficult, the best answer is to perform a regression-analysis on each block, punch the results into a deck of IBM cards, read the deck with the data analysis programs, and correct or normalize the data as it is read off of the magnetic tapes.

Figure 4 is a graph of three different range block transfer functions. Block 46 has a defective MOSFET which was not replaced before the data used for the graph was taken. The other two blocks have a linear transfer function, therefore a linear regression-analysis is a valid means of providing numbers for correction of block differences when the data is used.

Future plans include using the processor and the University of Illinois computing system to relate echo intensity levels to rainfall rates, thereby providing a means of remote rainfall measurement.

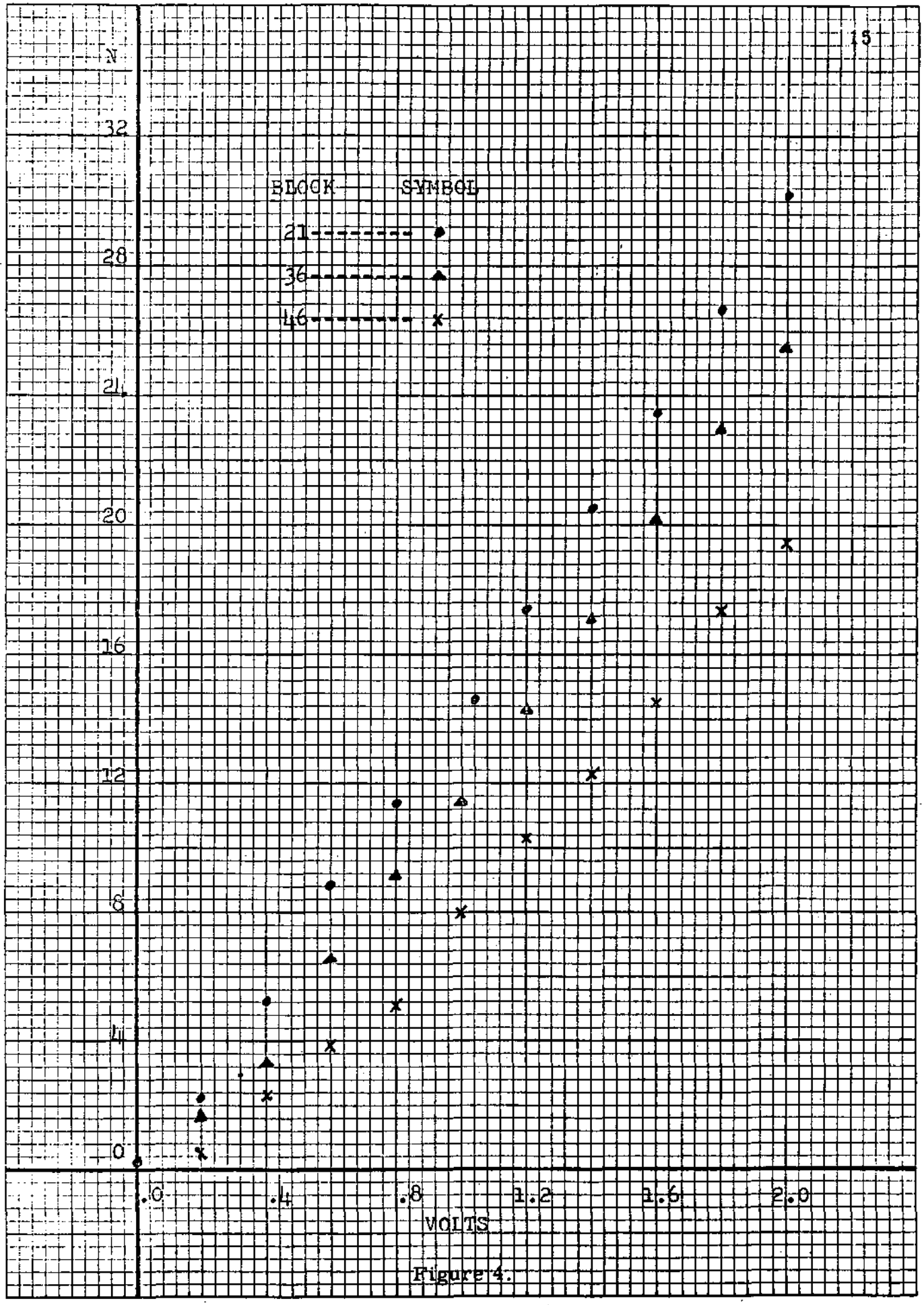

Figure 4.

APPENDIX

All the computer programs listed except the tape reader program have been modified to print the results in forms so that they could be included in this work.

Figure 5 is a listing of the Fortran program used to call an assembly subprogram that generates an inverted gray code to binary conversion table. When control is returned to the Fortran program, it prints the table, and the original program also punches a conversion deck to be used with programs calling the tape reader program. Figure 6 is the assembly program (TABLGN) used to generate the inverted conversion table. The reason the table is inverted is that the azimuth encoder could only be installed in the azimuth drive gear train in such a way as it turned counter-clockwise rather than clockwise in its normal mode. Figures 7 and 8 are the conversion table generated by the two preceding programs.

Figures 9, 10, 11, 12, 13, and 14 are a listing of the subprogram used to read the seven track tape recorded by the processor. Because the data is recorded with each character or byte representing one piece of data, it was not possible to read the tape with a Fortran program which is not capable of handling binary tapes with byte size data.

The first call to the tape reader must be to STUPTR (Figure 9). The listings in Figures 9 and 10 set up communication between the calling program and the tape reader, open the tape file, read the first record, store the housekeeping data in the calling program, and then cause a

```
IV G LEVEL  18                    MAIN                    DATE = 70256          02/06/

            INTEGER*2 TABLE(1024)
            CALL TABLGN(TABLE)
            N2=0
            WRITE(6,100)
            WRITE(6,104)
            DO 1 N=1,64
            N2=N2+16
            N1=N2-15
            N3=N1-1
            IF (N .EQ. 32) GO TO 2
            GO TO 1
    2       WRITE(6,100)
            WRITE(6,104)
    1       WRITE (6,103) N3, (TABLE(NP), NP=N1,N2)
  100       FORMAT('1',////////////,45X,'INVERTED GRAY CODE TO BINARY ',
           1   'CONVERSION TABLE')
  103       FORMAT(' ',15X,17I5)
  104       FORMAT('0',16X,'GRAY   +0   +1   +2   +3   +4   +5   +6',
           1          '   +7   +8   +9  +10  +11  +12  +13  +14  +15')
            END
```

Figure 5

```
STMT   SOURCE STATEMENT

    1 TABLGN   CSECT
    2          DS       0H
    3          USING    *,15              R15 IS TEMP BASE REG
    4          STM      14,12,12(13)      SAVE REGS IN CALLERS SVAR
    5          CNOP     0,4               GET A FW BD
    6          BALR     12,0              SETUP R 12 AS A BASE REG
    7          USING    *,12              R12 IS BASE REG
    8          DROP     15                R15 NOT BASE REG NOW
    9          LA       6,SVAR            R6=A(SVAR)
   10          ST       6,8(13)           A(OSVAR) IN TSVAR
   11          ST       13,4(6)           A(TSVAR) IN OSVAR
   12          LR       13,6              R13 = OSVAR
   13          L        2,0(0,1)          A(TABLE) TO R2
   14          SR       3,3               R3=0
   15          STH      3,0(0,2)          STORE 0
   16          LA       5,1023            R5=1023
   17          LA       4,1               R4=1
   18          LR       3,4               R3=1
   19 UNFN     LR       6,5               BINCOMP INTO R6
   20          SRL      6,1               SHIFT R6
   21          XR       6,5               GEN GRAY
   22          AR       6,6               R6*2
   23          STH      3,0(6,2)          ST BIN WITH GRAY AS ADDRESS
   24          AR       3,4               INC BIN
   25          BCT      5,UNFN            TEST FOR END OF TBL
   26 LEAVE    L        13,4(13)          LOAD THE ADDRESS OF CALLERS SVAR
   27          LM       14,12,12(13)      RESTORE REGS
   28          BR       14                RETURNING

   29 SVAR     DC       18F'0'
   30          END
```

Figure 6

GRAY	+0	+1	+2	+3	+4	+5	+6	+7	+8	+9	+10	+11	+12	+13	+14	+15
0	0	1023	1021	1022	1017	1018	1020	1019	1009	1010	1012	1011	1016	1015	1013	1014
16	993	996	996	995	1000	999	997	998	1008	1007	1005	1006	1001	1002	1004	1003
32	961	962	964	963	958	967	965	966	976	975	973	974	969	970	972	971
48	992	991	989	990	985	986	988	987	977	978	980	979	984	983	981	982
64	897	898	900	899	904	903	901	902	912	911	909	910	905	906	908	907
80	928	927	925	926	921	922	924	923	913	914	916	915	920	919	917	918
96	960	959	957	958	953	954	956	955	945	946	948	947	952	951	949	950
112	929	930	932	931	936	935	933	934	944	943	941	942	937	938	940	939
128	769	770	772	771	776	775	773	774	784	783	781	782	777	778	780	779
144	800	799	797	798	793	794	796	795	785	786	788	787	792	791	789	790
160	832	831	829	830	825	826	828	827	817	818	820	819	824	823	821	822
176	801	802	804	803	808	807	805	806	816	815	813	814	809	810	812	811
192	896	895	893	894	889	890	892	891	881	882	884	883	888	887	885	886
208	865	866	868	867	872	871	869	870	880	879	877	878	873	874	876	875
224	833	834	836	835	840	839	837	838	848	847	845	846	841	842	844	843
240	864	863	861	862	857	858	860	859	849	850	852	851	856	855	853	854
256	513	514	516	515	520	519	517	518	528	527	525	526	521	522	524	523
272	544	543	541	542	537	538	540	539	529	530	532	531	536	535	533	534
288	576	575	573	574	569	570	572	571	561	562	564	563	568	567	565	566
304	545	546	548	547	552	551	549	550	560	559	557	558	553	554	556	555
320	640	639	637	638	633	634	636	635	625	626	628	627	632	631	629	630
336	609	610	612	611	616	615	613	614	624	623	621	622	617	618	620	619
352	577	578	580	579	584	583	581	582	592	591	589	590	585	586	588	587
368	608	607	605	606	601	602	604	603	593	594	596	595	600	599	597	598
384	768	767	765	766	761	762	764	763	753	754	756	755	760	759	757	758
400	737	738	740	739	744	743	741	742	752	751	749	750	745	746	748	747
416	705	706	708	707	712	711	709	710	720	719	717	718	713	714	716	715
432	736	735	733	734	729	730	732	731	721	722	724	723	728	727	725	726
448	641	642	644	643	648	647	645	646	656	655	653	654	649	650	652	651
464	672	671	669	670	665	666	668	667	657	658	660	659	664	663	661	662
480	704	703	701	702	697	698	700	699	689	690	692	691	696	695	693	694

Figure 7 Inverted Gray Code to Binary Conversion Table

GRAY	+0	+1	+2	+3	+4	+5	+6	+7	+8	+9	+10	+11	+12	+13	+14	+15
496	673	674	676	675	680	679	677	678	688	687	685	686	681	682	684	683
512	1	2	4	3	8	7	5	6	16	15	13	14	9	10	12	11
528	32	31	29	30	25	26	28	27	17	18	20	19	24	23	21	22
544	64	63	61	62	57	58	60	59	49	50	52	51	56	55	53	54
560	33	34	36	35	40	39	37	38	48	47	45	46	41	42	44	43
576	128	127	125	126	121	122	124	123	113	114	116	115	120	119	117	118
592	97	98	100	99	104	103	101	102	112	111	109	110	105	106	108	107
608	65	66	68	67	72	71	69	70	80	79	77	78	73	74	76	75
624	96	95	93	94	89	90	92	91	81	82	84	83	88	87	85	86
640	256	255	253	254	249	250	252	251	241	242	244	243	248	247	245	246
656	225	226	228	227	232	231	229	230	240	239	237	238	233	234	236	235
672	193	194	196	195	200	199	197	198	208	207	205	206	201	202	204	203
688	224	223	221	222	217	218	220	219	209	210	212	211	216	215	213	214
704	129	130	132	131	136	135	133	134	144	143	141	142	137	138	140	139
720	160	159	157	158	153	154	156	155	145	146	148	147	152	151	149	150
736	192	191	189	190	185	186	188	187	177	178	180	179	184	183	181	182
752	161	162	164	163	168	167	165	166	176	175	173	174	169	170	172	171
768	512	511	509	510	505	506	508	507	497	498	500	499	504	503	501	502
784	481	482	484	483	488	487	485	486	496	495	493	494	489	490	492	491
800	449	450	452	451	456	455	453	454	464	463	461	462	457	458	460	459
816	480	479	477	478	473	474	476	475	465	466	468	467	472	471	469	470
832	385	386	388	387	392	391	389	390	400	399	397	398	393	394	396	395
848	416	415	413	414	409	410	412	411	401	402	404	403	408	407	405	406
864	448	447	445	446	441	442	444	443	433	434	436	435	440	439	437	438
880	417	418	420	419	424	423	421	422	432	431	429	430	425	426	428	427
896	257	258	260	259	264	263	261	262	272	271	269	270	265	266	268	267
912	288	287	285	286	281	282	284	283	273	274	276	275	280	279	277	278
928	320	319	317	318	313	314	316	315	305	306	308	307	312	311	309	310
944	289	290	292	291	296	295	293	294	304	303	301	302	297	298	300	299
960	384	383	381	382	377	378	380	379	369	370	372	371	376	375	373	374
976	353	354	356	355	360	359	357	358	368	367	365	366	361	362	364	363
992	321	322	324	323	328	327	325	326	336	335	333	334	329	330	332	331
1008	352	351	349	350	345	346	348	347	337	338	340	339	344	343	341	342

Figure 8 Inverted Gray Code to Binary Conversion Table

```
 2          PRINT   NOGEN
 3 STUPTR   CSECT
 4 BEGIN    STM     14,12,12(13)    SAVE MAIN REGS
 5          BALR    12,0            **SETUP R12
 6          USING   *,12            **EQ BASE REG
 7 BASEA    LA      6,SVAR          R6 EQ A(SVAR)
 8          ST      6,8(13)         SAVE A(SVAR) IN MSVAR
 9          ST      13,4(6)         SAVE A(MSVAR) IN SVAR
10          LR      13,6            R13 EQ A(SVAR)

12 PARADD  L       9,0(1)          R9 EQ A(TBL)
13         LA      10,2048(9)      R10 EQ A(DTA)
14         LH      6,0(10)         LOAD DTA BLOCK SIZE
15         LA      6,0(6,10)       R6 EQ (A(HOUSE KEEPING DATA))
16         LH      8,2(10)         R8 EQ NUMBER OF DATA ROWS
17         SR      11,11           INITILIZE RC EQ 0
18         LA      4,4             INCR FOR DTA BXLE LOOP
19         SR      7,7             SET DTA INDEX AT 0

21 OPEN    LA      1,OP
22         SVC     19

24         LA      1,RDTA
25         LA      0,REC
26         L       15,48(0,1)
27         BALR    14,15

29 TIME    MVC     NT,REC          LOAD NT
30         MVC     NOI,REC+13      UPDATE OFFSET AND INCR
31         MVC     OT(9),NT        LOAD OT-OOI

33 HKDTA   MVC     AHSK(9),NT      MOVE TIME-OFFSET-INCR
34         MVC     HSK+1(9),AHSK   SPLIT BYTES
35         NC      HSK(9),ZSPLT    CONV TO WORDS/2
36         NC      AHSK(9),ZSPLT   CONV TO WORDS/2

38 DAYS    LH      1,HSK           LOAD D
39         LA      2,0(1,1)        R2 EQ 2*D
40         LA      1,0(2,2)        R1 EQ 4*D
41         AR      1,1             R1 EQ 8*D
42         AR      1,2             R1 EQ 10*D
43         AH      1,AHSK          R1 EQ 10*D+A
44         LA      2,0(1,1)
45         LA      1,0(2,2)
46         AR      1,1
47         AR      1,2
48         AH      1,HSK+2
49         STH     1,10(6)         STORE DAYS
```

Figure 9

```
STMT   SOURCE STATEMENT

   51 HRS       LH          1,AHSK+2
   52           LA          2,0(1,1)
   53           LA          1,0(2,2)
   54           AR          1,1
   55           AR          1,2
   56           AH          1,HSK+4
   57           STH         1,12(6)          STORE HRS

   59 MINS      LH          1,AHSK+4
   60           LA          2,0(1,1)
   61           LA          1,0(2,2)
   62           AR          1,1
   63           AR          1,2
   64           AH          1,HSK+6
   65           STH         1,14(6)          STORE MINS

   67           LH          1,AHSK+6
   68           STH         1,16(6)          STORE OS

   70           LH          1,HSK+8
   71           STH         1,18(6)          STORE INCR

   73           LA          1,TPRDR
   74           BALR        12,1
   75           USING       *,12
```

Figure 10

```
 77             ENTRY    RECALL
 78 RECALL      STM      14,12,12(13)     SAVE MAIN REGS
 79             LR       12,15
 80 BASER       LA       6,SVAR           R6 EQ A(SVAR)
 81             ST       6,8(13)          ST A(SVAR) IN MSVAR
 82             ST       13,4(6)          ST A(MSVAR) IN SVAR
 83             LR       13,6             R13 EQ A(SVAR)
 84             LM       4,11,TEMPREG     RESTORE R4 THRU R11

 86 TPRDR       CLC      OT(9),NT         **IF NT EQ OT
 87             BC       8,INT            **GO TO INT
 88             MVC      OT(9),NT         LOAD NEW TIME-OFFSET-INCR
 89             LTR      11,11            **IF R11 EQ 0
 90             BC       8,READ           **GO TO READ

 92 DHKDTA      MVC      AHSK(9),NT       MOVE TIME-OFFSET-INCR
 93             MVC      HSK+1(9),AHSK    SPLIT BYTES
 94             NC       HSK(9),ZSPLT     CONV TO WORDS/2
 95             NC       AHSK(9),ZSPLT    CONV TO WORDS/2

 97             LH       1,HSK            LOAD 0
 98             LA       2,0(1,1)
 99             LA       1,0(2,2)
100             AR       1,1
101             AR       1,2
102             AH       1,AHSK           R1 EQ 10*D+A
103             LA       2,0(1,1)
104             LA       1,0(2,2)
105             AR       1,1
106             AR       1,2
107             AH       1,HSK+2
108 DDAYS       STH      1,0(6)           STORE DAYS

110 DHRS        LH       1,AHSK+2
111             LA       2,0(1,1)
112             LA       1,0(2,2)
113             AR       1,1
114             AR       1,2
115             AH       1,HSK+4
116             STH      1,2(6)           STORE HRS

118 DMINS       LH       1,AHSK+4
119             LA       2,0(1,1)
120             LA       1,0(2,2)
121             AR       1,1
122             AR       1,2
123             AH       1,HSK+6
124             STH      1,4(6)           STORE MINS
```

Figure 11

```
126 OTS     LH      1,AHSK+6
127         STH     1,6(6)          STORE OS

129 OUNC    LH      1,HSK+8
130         STH     1,8(6)          STORE INCR

132         MVC     OT(9),NT        UPDT TM-OFS
133         LA      1,2             R1 EQ 2
134         STH     1,24(6)         SET NEW TIME-OFFSET FLAG

136         BC      15,LEAVE        GO TO MAIN

138 INT     MVC     AZ,REC+9        LOAD AZ
139 AZM     NC      AZ,ZERO         TR ZEROS
140         LH      3,AZ            LOAD R3 WITH AZ
141         NI      AZ,X'00'        AZ EQ 0Z
142         SH      3,AZ            R3 EQ A0
143         SRL     3,3             R3 EQ A+S80
144         AH      3,AZ            R3 EQ GRAZ
145         AR      3,3             R3 EQ GRAZ*2
146         LH      1,0(3,9)        R1 EQ BINAZ

148         BC      15,INCRC
149 AZTST   L       2,SECTC         R2 EQ SECT CNTR
150         SR      2,1             R2 EQ AZ DIFF
151         LPR     2,2             R2 EQ MAG OF R2
152         C       2,SECTW         **IF AZ IS NOT OVER NETWORK
153         BC      11,READ         **GO TO READ

155 INCRC   STH     1,0(7,10)       STORE AZ
156         LA      11,1(11)        INCREMENT RC
157 INTSEC  MVC     AZ,REC+7        LOAD SECS
158         NC      AZ,ZERO
159         LH      3,AZ            R3 EQ SECS
160         NI      AZ,X'00'        AZ EQ 0C
161         SH      3,AZ            R3 EQ S0
162         SRL     3,8             R3 EQ S
163         STH     3,2(7,10)       STORE S
164         LH      3,AZ            R3 EQ C
165         STH     3,4(7,10)       STORE C
166         LA      7,6(7)          INCR DTA INDEX
167 SEPAR   MVC     AREC+14(50),REC+15
168         NC      AREC+14(50),ZSPLT
169         NC      REC+14(50),ZSPLT
170         LA      5,96(7)         BXLE TEST R7, R4, R5
171         LA      3,14            SET REC PNTR
172 VIDEO   LH      2,REC(3)        LOAD DATA
173         STH     2,0(7,10)       STORE DATA
174         LH      2,AREC(3)       LOAD DATA
```

Figure 12

```
STMT   SOURCE STATEMENT

 175           STH       2,2(7,10)       STORE DATA
 176           LA        3,2(3)          INC REC PNTR
 177           BXLE      7,4,VIDEO

 179 READ      LA        1,RDTA
 180           LA        0,REC
 181           L         15,48(0,1)
 182           BALR      14,15

 184           MVC       NT,REC          UPDT TM
 185           MVC       NOI,REC+13      UPDATE OFFSET-INCRE
 186           CR        11,8            **IF RC LT TEN
 187           BC        4,TPRDR         **GO TO TPRDR
 188           BC        15,LEAVE        GO TO MAIN

 190 ENDF      LA        2,2             **SET END OF
 191           ST        2,20(6)         **DATA FLAG

 193 CLOSE     LA        1,CLS
 194           SVC       20

 196 LEAVE     STH       11,22(6)        STORE RECORD COUNT
 197           SR        7,7             RESET DTA INDEX
 198           SR        11,11           RESET RC
 199           STM       4,11,TEMPREG    SAVE REGS

 201           L         13,4(13)        GET A(MSVAR)
 202           LM        14,12,12(13)    RESTORE MAIN REGS
 203           BCR       15,14           RETURNING
```

Figure 13

```
STMT   SOURCE STATEMENT

  205 SVAR      DS          18F
  206 TEMPREG   DS          16F
  207 AREC      DS          CL68
  208 REC       DS          CL65
  209           DC          X'000000'
  210 ZERO      DC          4X'1F'
  211 ZSPLT     DC          34X'001F'
  212 OT        DS          CL7
  213 OOI       DS          CL2
  214 NT        DS          CL7
  215 NOI       DS          CL2
  216 AZ        DS          H
  217 HSK       DS          CL10
  218 AHSK      DS          CL10
  219 SECTC     DC          F'830'
  220 SECTW     DC          F'117'
  221 CLS       DC          AL1(128)
  222           DC          AL3(RDTA)
  223 OP        DC          AL1(128)
  224           DC          AL3(RDTA)
  225 RDTA      DCB         DSORG=PS,MACRF=GM,LRECL=65,BLKSIZE=65,RECFM=F,
                      DEVD=TA,DEN=1,TRTCH=E,DDNAME=RDTA,EODAD=ENDF,EROPT=ACC
  282           END
```

Figure 14

branch to TPRDR (Figure 11). This section (Figures 11, 12, 13, and 14) transfers video and translated azimuth, data to the calling program, updates the housekeeping data, and flags the end of data condition. This section returns to the calling program when the data buffer the calling program provides is full, or when the end of data is reached.

Figures 15 and 16 is a listing of the Fortran program used to calculate the linear regression-analysis shown in Figures 17 and 18. The voltage levels used to calibrate the tape reader were entered into the program in Figure 15, line 2. The program then called the tape reader and then was able to match voltage input to the processor, and number output from the processor.

Figures 19, 20, 21, and 22 are uncorrected sample data of actual thunder storms recorded with . 5 mile range blocks.

```
      COMMON TBL,DTA,HSK,AHSK,ENFI,RC,NT
      REAL AVG(24,50)
      INTEGER*2 TBL(1024),DTA(5300),HSK(5),AHSK(5),ENFI,RC,NT
      INTEGER X(12)/20,18,16,14,12,10,8,6,4,2,0,1/
      INTEGER TRC/0/,NX/0/,SKIP/1/
      REAL*8 SUM(250)/250*0./,DX,DY,DXDY,R,RN,SYX,NY,NXX,SY,SYY,
     1       SSYY,SSY,SX,SXX,AA,AB
      DTA(2)=100
      DTA(1)=DTA(2)*106
      ENFI=1
      NT=1
      DO 900 N=1,64
900   READ (5,100) NA, NB, (TBL(NC),  NC = NA, NB)
      NXT=12
      CALL STUPTR(TBL)
      GO TO 1
3     CALL RECALL
1     IF(RC .EQ.0) GO TO 2
      IF(SKIP .EQ. 2) GO TO 4
      IF(RC .GT. 50) RC=50
      TRC=TRC+RC
      LN=RC*53
      IF(NT .EQ. 1) SKIP=2
      NX=NX+1
      NXX=X(NX)
      NXX=NXX/10.
      SN=RC
      DO 5 N=3,52
      SY=0
      SYY=0
      DO 6 NA=1,LN,53
      NY=DTA(N+NA)
      SY=SY+NY
6     SYY=SYY+NY*NY
      NA=(N-3)*5+1
      SUM(NA)=SUM(NA)+SY
      SUM(NA+1)=SUM(NA+1)+SYY
      SUM(NA+2)=SUM(NA+2)+NXX*SY
      SUM(NA+3)=SUM(NA+3)+NXX*SN
      SUM(NA+4)=SUM(NA+4)+NXX*NXX*SN
      AVG(NX,N-2)=SY/SN
      SY=DABS((SYY-SY*(SY/SN))/(SN-1.))
5     AVG(NX+12,N-2)=DSQRT(SY)
4     IF(NX .EQ. NXT) GO TO 8
      IF(NT .EQ. 2) SKIP=1
2     IF(ENFI .EQ. 1) GO TO 3
8     WRITE(6,102)
      WRITE(6,103) AVG
      WRITE(6,104)
      DO 7 NA=1,50
      N=5*(NA-1)+1
      SY=SUM(N)
      SYY=SUM(N+1)
```

Figure 15

```
      SXY=SUM(N+2)
      SX=SUM(N+3)
      SXX=SUM(N+4)
      SN=TRC
      DX=SN*SXX-SX*SX
      DY=SN*SYY-SY*SY
      RN=SN*SXY-SX*SY
      DXDY=DABS(DX*DY)
      R=RN/DSQRT(DXDY)
      AA=(SY*SXX-SX*SXY)/DX
      AB=RN/DX
      BB=RN/DY
      BA=(SX*SYY-SY*SXY)/DY
      SSYY=(SXX-BA*SX-BB*SXY)/(SN-2)
      SSYY=DABS(SSYY)
      SSYY=DSQRT(SSYY)
      SSY=(SYY-AA*SY-AB*SXY)/(SN-2)
      SSY=DABS(SSY)
      SSY=DSQRT(SSY)
      WRITE(7,106) NA,AA,AB,SSY,BA,BB,SSYY,R
      WRITE(6,105) NA,AA,AB,SSY,BA,BB,SSYY,R
      IF(NA .NE. 25) GO TO 7
      WRITE(6,104)
    7 CONTINUE
  100 FORMAT(18I4)
  101 FORMAT(18I4)
  102 FORMAT('1AVERAGE OUTPUT FOR EACH GATE AT EACH LEVEL',/,
     1       ' STANDARD DEVIATION FOR THAT GATE AT THAT LEVEL',//)
  103 FORMAT('0',12F10.3,/,' ',12F10.3)
  104 FORMAT('1',15X,'GATE    A0        A1        SYX       B0',
     1       '        B1       SXY       R',/)
  105 FORMAT(' ',16X,I2,1X,7F9.4)
  106 FORMAT(I4,10F10.5)
      END
```

Figure 16

GATE	A0	A1	SYX	B0	B1	SXY	R
1	-1.6323	12.5250	0.9033	0.1398	0.0789	0.0717	0.9940
2	-0.8888	14.4023	0.7067	0.0665	0.0690	0.0489	0.9972
3	-0.4749	15.0864	0.7803	0.0370	0.0659	0.0516	0.9969
4	-0.4315	14.7818	0.6330	0.0330	0.0674	0.0427	0.9979
5	-0.5817	15.2613	0.6997	0.0424	0.0652	0.0457	0.9976
6	-0.9434	13.9478	0.6449	0.0719	0.0713	0.0461	0.9975
7	0.1353	14.3744	0.7640	-0.0033	0.0691	0.0530	0.9967
8	-0.6904	14.8238	0.7278	0.0515	0.0671	0.0490	0.9972
9	-1.1791	13.3937	0.8032	0.0950	0.0740	0.0597	0.9958
10	-1.0655	13.6564	0.7975	0.0847	0.0726	0.0582	0.9961
11	-0.9183	14.3117	0.6904	0.0688	0.0695	0.0481	0.9973
12	-0.9368	13.8777	0.7698	0.0736	0.0715	0.0553	0.9964
13	-0.8518	14.4110	0.7141	0.0640	0.0690	0.0494	0.9972
14	-0.7005	14.3771	0.6694	0.0531	0.0692	0.0464	0.9975
15	-0.8242	14.3522	0.6673	0.0618	0.0693	0.0464	0.9975
16	-0.6387	13.4184	0.6857	0.0529	0.0741	0.0509	0.9970
17	-0.4055	14.7645	0.6391	0.0314	0.0674	0.0432	0.9978
18	-0.5973	14.5736	0.6926	0.0456	0.0683	0.0474	0.9974
19	-0.3440	14.8224	0.6419	0.0271	0.0672	0.0432	0.9978
20	-0.7858	14.3630	0.7176	0.0597	0.0692	0.0498	0.9971
21	-0.5566	14.8504	0.6038	0.0409	0.0671	0.0406	0.9981
22	-0.6769	14.5282	0.7103	0.0515	0.0685	0.0488	0.9972
23	-0.4174	14.7648	0.6446	0.0322	0.0674	0.0436	0.9978
24	-1.4588	14.0545	0.8291	0.1104	0.0706	0.0588	0.9960
25	-1.0311	13.9327	0.8345	0.0810	0.0712	0.0597	0.9959

Figure 17 Linear Regression Analysis for Fifty Gates

GATE	A0	A1	SYX	B0	B1	SXY	R
26	-1.1210	13.3812	0.7720	0.0902	0.0742	0.0575	0.9962
27	-0.7945	14.3148	0.7626	0.0612	0.0694	0.0531	0.9967
28	-0.8263	14.3527	0.7088	0.0625	0.0693	0.0493	0.9972
29	-0.6052	14.8722	0.5974	0.0440	0.0670	0.0401	0.9981
30	-0.8792	14.2424	0.6722	0.0662	0.0699	0.0471	0.9974
31	-0.6854	13.8833	0.6585	0.0539	0.0717	0.0473	0.9974
32	-0.8386	13.4796	0.7974	0.0692	0.0736	0.0589	0.9960
33	-0.2611	14.4318	0.7532	0.0238	0.0689	0.0520	0.9968
34	-0.9336	13.8292	0.8350	0.0747	0.0717	0.0601	0.9958
35	-0.9434	12.9046	0.7329	0.0795	0.0769	0.0566	0.9963
36	-1.0893	12.9632	0.7612	0.0907	0.0765	0.0585	0.9960
37	-1.3637	12.3463	0.8481	0.1193	0.0801	0.0683	0.9946
38	-1.0908	13.8585	0.8516	0.0861	0.0715	0.0612	0.9956
39	-1.1756	13.0835	0.7722	0.0966	0.0758	0.0588	0.9960
40	-1.2676	12.3019	0.8989	0.1131	0.0803	0.0726	0.9938
41	-0.5026	14.1452	0.7705	0.0416	0.0702	0.0543	0.9966
42	2.4028	12.7375	0.6691	-0.1815	0.0780	0.0524	0.9968
43	-1.5975	12.7973	0.8828	0.1336	0.0773	0.0686	0.9945
44	-1.3928	12.4210	0.8798	0.1215	0.0796	0.0704	0.9942
45	-1.8445	11.0301	1.0027	0.1815	0.0890	0.0900	0.9905
46	-1.4528	9.8553	0.8481	0.1606	0.0997	0.0853	0.9915
47	-1.5514	10.6087	0.8595	0.1579	0.0928	0.0804	0.9925
48	-0.9976	13.7091	0.7951	0.0794	0.0724	0.0578	0.9961
49	-1.7387	7.9877	1.0223	0.2436	0.1206	0.1256	0.9815
50	0.6163	7.7770	0.8412	-0.0526	0.1252	0.1067	0.9867

Figure 18 Linear Regression Analysis for Fifty Gates

```
DAY   HR   MIN   OFFSET   INCREMENT
246   12    51     1          3

AZIMUTH   SECS   VIDEO(1) THROUGH VIDEO(50)
 247.50    08    ------1----------1------1----------------2
 248.91    08    ------1--------------1---1----------1-2
 250.31    08    ------1-------1231----------1----------------1-2
 251.72    08    ------1------13542-----------------------------2
 253.13    08    ----111-----112683----------------------------2
 254.53    08    ---1222-1-11445652----------------------------2
 255.94    08    ----34314368A8741-----------------------------1
 257.34    08    --112332558A8641------------------------------2
 258.75    08    -123224324684 21------------------------------1
 260.16    08    -121213311452---1-----------------------------2
 261.56    08    --121-2112111---1-----1-----------------------2
 262.97    09    ---111222431-----------------1---------------2
 264.38    09    --1---466431-----------------------------------2
 265.78    09    24451-4751-------------------------------------2
 267.19    09    12543-221--------1-----------------------------2
 268.59    09    --222-----------------------------------------2
 270.00    09    ----342----------1----------------1----------2
 271.41    09    ----242--------------------1----1--------------2
 272.81    09    ------1-------------1-----11---1--------------2
 274.22    09    ------1--------------1----11-1-1--------------2
 275.63    09    ------1----------1-------1332--1---------------1
 277.03    09    ------1--------1------1---1234341-------------2
 278.44    09    ------1---------------1---1488532-------------1
 279.84    09    -----11--------------1-12469521---------------2
 281.25    09    ------1--------------123576631-1--------------2
 282.66    09    ------1-------------122458742----------1-------1
 284.06    09    ------1----------1---2333321-----------------2
 285.47    09    ------1--------1----112111111---11------1-------2
 286.88    09    ------1--------------1-11112---1--------------2
 288.28    09    ------1-------1-------1-22111----1------1-------2
 289.69    09    ------1----------1---129731-------------------2
 291.09    09    ------1-------1-------25853---------------1-----2
 292.50    10    ------1--------------1121111----1--------342----2
 293.91    10    ------1--------------------1---1--------233211-2
 295.31    10    ------1----------1--------1---1----------11223-2
 296.72    10    ------1----------1----------1-1------1----1-1-2
 298.13    10    ------1----------1----------1-1------1-------2
 299.53    10    ------1----------------------1---1------1-------2
 300.94    10    ------1------------------1-----1------1-------2
 302.34    10    ------1----------1-----1-----1-----1-1-------2
 303.75    10    -12---1----------1-------1----------1--------2
 305.16    10    --1---1----------------1------1--------------3
 306.56    10    ------1--------------1---1-1---1------1------1-2
 307.97    10    ------11---------------1------1------1-------2
 309.38    10    ------1----------------1------1-------------113
 310.78    10    ------1------1------1--------11------1------2-3
 312.19    10    ------1----------------------1-------1------2-2
 248.91    20    ------1--------------------1----------------1-2
```

Figure 19

```
246  12    54     1          3

AZIMUTH   SECS  VIDEO(1) THROUGH VIDEO(50)
 251.72    08   ------1---111---------------1-----------------2
 253.13    08   ------1---14421-------------------------------2
 254.53    08   ------1---12561-------------------------1-------2
 255.94    08   221--11-5423641-------------------------------2
 257.34    08   14323555664221--------------------------------2
 258.75    08   -342565765511---------------------------------2
 260.16    08   -24344357331----------------------------------2
 261.56    08   -123313461------------------------------------2
 262.97    09   --1121221---------1---------------------------2
 264.38    09   --111232----------------------1---------------1
 265.78    09   --243365----------------1-----1---------------2
 267.19    09   --778863--------------------------------------3
 268.59    09   2-27A64---------------------------------------2
 270.00    09   1212432---------------------------------------2
 271.41    09   -1112-1---------------------------------------2
 272.81    09   -3421-1-------------1---------11------1-------2
 274.22    09   -4971-1-------------1-----------------1-------2
 275.63    09   -1221-1-----------------------1---1-----------2
 277.03    09   ------1-----------1----1331---------1---------2
 278.44    09   ----1-1---------------134311---1--------------2
 279.84    09   -----11------1-------1-15631---1--------------2
 281.25    09   ------1----------1---1134841-----------------2
 282.66    09   ------1----------1122477631------------------2
 284.06    09   ------1---------1---24778631-----------------2
 285.47    09   ------1----------11234443211-----------------2
 286.88    09   ------1----------1122311-1-------------------2
 288.28    09   ------1---------1--11211-1-----1------1-------2
 289.69    09   ------1----------1--113-1-----1--------------2
 291.09    09   ------1-------1------341------1-1------------2
 292.50    09   ------1------1----1--3874------1--------------2
 293.91    10   ------1-------------2542--1----1------1231-----2
 295.31    10   ------11------------1211-1-----1------3332-----2
 296.72    10   ------1-------------1----1----1------121221---2
 298.13    10   ------1----------1---1---1-----1----1--1--1-1--2
 299.53    10   ------1----------1---1---1-----1------1-------2
 300.94    10   ------1-----------------1-----1------1-------2
 302.34    10   ------1-----1-----1-----------11----11-1-------2
 303.75    10   --2---1------1-------1---------1----1111------2
 305.16    10   --1---1-------------1---1-----11------1-------2
 306.56    10   ------1----1------1---------1--1------1-------2
 307.97    10   ------1----------1----1---1-----1------1-------2
 309.38    10   ------1-------------1---------1-1-----1------2-2
 310.78    10   ------1---1-----1-11-------1---1------1------2-3
 312.19    10   ------1-----------------1-----1------1------2-2
 313.59    10   ------1------1------1---------11------1------2-2
 315.00    10   ------2----------1----1---1-----1------1------2-3
 316.41    10   ------1----------1------111---1----1--1------2-3
 317.81    10   --1---1----------1-1---1-1---1------1------1-2
```

Figure 20

```
DAY   HR   SIM   OFFSET   INCREMENT
266   12   56     1          3

ACTUAL TIME   SECS   VIDEO(1) THROUGH VIDEO(50)
 247.50        08    ------1--------------1----------1-----1-------2
 248.91        08    ------1----------------1-------1---------------2
 250.31        08    ------1-------------1-------1---1---------------2
 251.72        08    ------1--------------------1---1---------------2
 253.13        08    ------1-131----------------1---1---------------2
 254.53        08    ------1-232--------------1-----1---------------2
 255.94        08    -----12-1264-------------------------------------2
 257.34        08    --11-4631472---------------1-----------------1-2
 258.75        08    -2554586311----------------------------------------2
 260.16        08    145444663------------------------------------------2
 261.56        08    245436932------------------------------------------2
 262.97        09    23233352-------------------------------1--------2
 264.38        09    -11-1131-------------------1-----------------------2
 265.78        09    --121-1----------------------1-1-----------------2
 267.19        09    -112451-------------------------1--------------2
 268.59        09    3556842--------------------------------------------2
 270.00        09    3975721--------------------------------------------2
 271.41        09    -3564-1--------------------------------------------2
 272.81        09    -1331-1----------------------1--------1--------2
 274.22        09    ---1--1--------------1--------1--------1--------2
 275.63        09    21----1---------1----------------------1--------2
 277.03        09    43----1-------------1-1-----1-----------------2
 278.44        09    -1----1-----------1---223311--------------------2
 279.84        09    -----21--------------1477321--------------------2
 281.25        09    ------1---------1-----47A6421-------------------2
 282.66        09    ------1------1----1---34A8411---1---------------2
 284.06        09    ------1-------------2377754---------------------2
 285.47        09    ------1-----------1244643211--------------------2
 286.88        09    ----1-1-----------1224431-------1---------------2
 288.28        09    ------1-------1---1111211-------1-------1--------2
 289.69        09    ------1--------1--11111---------1-1-----1--------2
 291.09        09    ------1--------1------1---------11------1--------2
 292.50        10    ------1----------2---13----------1-----1--------2
 293.91        10    ------1------------144---------1---------------2
 295.31        10    ------1------------137621--------------21-------2
 296.72        10    ------1----------1-122-----1---1------2421------2
 298.13        10    ------1--------------1-1-------11------2112-----2
 299.53        10    ----1-1---------------1----1---1-------1-11-----2
 300.94        10    ------1-------------------1----1-------1--------2
```

Figure 21

DAY	HR	MIN	OFFSET	INCREMENT
246	12	59	1	3

AZIMUTH	SECS	VIDEO(1) THROUGH VIDEO(50)
253.83	32	------1----------1----1----------
255.23	32	----111----------1--------11----------
256.64	32	----232-------1----------1----1----------
258.05	32	---111231----------1----1----------
259.45	32	-3331483----------1----------
260.86	32	13542241----------1----1----------
262.27	33	12652-1----------1----------
263.67	33	-28531----------1----------
265.08	33	12651-1----------1----------
266.48	33	-2351-1----------1----1----------
267.89	33	-1211-1----------1----1----------
269.30	33	-11---1----------1----1----------
270.70	33	-221--1----------1----1----------
272.11	33	-2421-1----------1-------
273.52	33	-42---1----------1----------
274.92	33	241----------1----------
276.33	33	-2----1----------1----------1----1----------
277.73	33	------1----------1----------1-1----------
279.14	33	------1---------1----1---------1----------
280.55	33	-----11----------1----1----1----------
281.95	33	------1----------245511----------
283.36	33	------1----------149A721----------
284.77	33	------1----------1378841----------
286.17	33	------1----------1353A63----------
287.58	33	------1---1-----124566632----------
288.98	33	------1---------3444432----------1----------
290.39	33	------1---------1332211----1----1----------
291.80	33	------1---------12,1112---------1----------
293.20	34	------1---------1111111-----1---1----------
294.61	34	------1---------1-11111----1----1----------
296.02	34	------1----------41-----1----1----------
297.42	34	------1-------1---11521-------1-11----------
298.83	34	-----1----------2333-----1----1-----11----------
300.23	34	------1----------11111-----1---1----1----------
301.64	34	------1----------1----1----------
303.05	34	------1----------1----------1----1--1----------
304.45	34	--11--1---------1----1---1-----1----------
305.86	34	------1---------1---------1----1----------
307.27	34	------1----------1----1----------
308.67	34	------1---1-----1-1---1-----1--1----------
310.08	34	------1---------1-1---1----1----1----------
311.48	34	------1---------1-11---------1--1----------
246.09	44	-1----1----------1-------1----------
247.50	44	------1----------1---------1-1----------
248.91	44	------1----------1------1--1----------
250.31	44	------1----------1-1-1------
251.72	44	------1---------1-----1----------
253.13	44	------1----------1-----1-1---1------

Figure 22

LIST OF REFERENCES

1. Austin, P. M., Application of Radar to Measurement of Surface Precipitation, ECOM-0319-F, United States Army Electronics Command, Fort Monmonta, N. J., March, 1969.

2. Wallace, P. R., Interpretation of the Fluctuating Echo from Randomly Distributed Scatters: Part 1, McGill University, Research Report MW-6, Air Force Cambridge Research Center, AMC, December, 1951.

3. Smith, P. L., Interpretation of the Fluctuating Echo from Randomly Distributed Scatters: Part 3, McGill University, Research Report MW-39, Air Force Cambridge Research Center, AMC, December, 1964.

4. RCA DATA BOOK, File No. 138, Radio Corporation of America, Harrison, New Jersey.

5. Turner, R. J., Zeners Cut Corners in MOS Gate Driver, Electronics, Vol. 43, No. 13, June 22, 1970.

6. Crawford, R. H., MOSFET in Circuit Design, McGraw-Hill Book Company, New York, New York, 1967.

7. Ridenour, L. N., MIT Radiation Laboratory Series, Vols. 13 and 24, McGraw-Hill Book Company, New York, New York, 1951.

8. Terman, F. E., Electronic and Radio Engineering, McGraw-Hill Book Company, New York, New York, 1955.

9. Mrazek, D., Low Voltage Offers New Jobs for MOS Commutators, Electronics, Vol. 43, June 8, 1970.

DISTRIBUTION LIST

DEPARTMENT OF DEFENSE

2 Defense Documentation Center
Attn: DDC-TCA
Cameron Station (Bldg 5)
Alexandria, Virginia 22314

1 Director of Defense Research £ Engineering
Attn: Technical Library
Room 3E-1039, The Pentagon
Washington, D. C. 20301

1 Joint Chiefs of Staff
Attn: Special Assistant
Environmental Services
Washington, D. C. 20301

1 Defense Intelligence Agency
Attn: DIAAP-10A2
Washington, D. C. 20301

1 Director, Defense Atomic Support Agency
Attn: Technical Library
Washington, D. C. 20305

DEPARTMENT OF THE NAVY

1 Naval Ships Systems Command
Attn: Code 20526 (Technical Library)
Main Navy Bldg., Room 1528
Washington, D. C. 20325

2 Director, U. S. Naval Research Laboratory
Attn: Code 2027
Washington, D. C. 20390

1 Commanding Officer and Director
U. S. Navy Electronics Laboratory
Attn: Library
San Diego, California 92152

1 Commander
U. S. Naval Ordnance Laboratory
Attn: Technical Library
White Oak, Silver Spring,
Maryland 20910

1 Officer in Charge
Navy Weather Research Facility
Bldg R-48, Naval Air Station
Norfolk, Virginia 23511

1 Commandant, Marine Corps
HQ, U. S. Marine Corps
Attn: Code A04C
Washington, D. C. 20380

1 Commandant, Marine Corps
HQ, U. S. Marine Corps
Attn: Code A02F
Washington, D. C. 20380

1 Marine Corps Development £ Educ. Command
Development Center, Attn: C-E Div.
Quantico, Virginia 22134

1 Commander
U. S. Naval Weapons Laboratory
Attn: KXR
Dahlgren, Virginia 22448

1 Commander, Naval Air Systems Command
Meteorological Division (Air-540)
Washington, D. C. 20360

1 Commander
Naval Weather Service Command
Washington Navy Yard (Bldg 200)
Washington, D. C. 20390

DEPARTMENT OF THE AIR FORCE

1 Air Force Cambridge Research Labs
Attn: CREU
L. G. Hanscom Field
Bedford, Massachusetts 01730

1 Air Force Cambridge Research Labs
Attn: CREW
L. G. Hanscom Field
Bedford, Massachusetts 01730

1 Air Force Cambridge Research Labs
Attn: CRH
L. G. Hanscom Field
Bedford, Massachusetts 01730

1 Air Force Cambridge Research Labs
Attn: CRER
L. G. Hanscom Field
Bedford, Massachusetts 01730

1 Electronic Systems Div. (ESSIE)
L. G. Hanscom Field
Bedford, Massachusetts 01730

2 Electronic Systems Division (ESTI)
L. G. Hanscom Field
Bedford, Massachusetts 01730

1 RFC0N Central/AVRS
AF Avionics Laboratory
Wright-Patterson AFB, Ohio 45433

1 HQ, Air Weather Service
Attn: AWVAS/TF (R. G. Stone)
Scott Air Force Base, Illinois 62225

1 U. S. Air Force Security Service
Attn: TSG
San Antonio, Texas 78241

1 Armament Development & Test Center
Attn: ADBPS-12
Eglin Air Force Base, Fla. 32542

1 HQ, Air Force Systems Command
Attn: SCTSE
Andrews AFB, Maryland 20331

1 Commander
29th Weather Squadron (MAC)
Attn: 290V
Richards-Gebaur AFB, Mo. 64030

1 Air Force Weapons Laboratory
Attn: WLIL
Kirtland AFB, New Mexico 87117

1 Commanding Officer
USAF Environmental Technical Applications Center
Attn: Tech Info Section
Bldg. 159, Navy Yard Section
Washington, D. C. 20333

DEPARTMENT OF THE ARMY

1 Office of Assistant Chief of Staff for DS-SSS
Department of the Army
Room 3C466, The Pentagon
Washington, D. C. 20315

1 Assistant Chief of Staff for Force Development
CRR Nuclear Operations Directorate
Department of the Army
Washington, D. C. 20310

1 Office, Assistant Secretary of the Army (R 6 D)
Attn: Assistant for Research
Room 3-E-373, The Pentagon
Washington D. C. 20310

2 Chief of Research and Development
Department of the Army
Washington, D. C. 20315

1 Chief of Research and Development
Department of the Army
Attn: CRD/M
Washington, D. C. 20310

1 Commanding General
U. S. Army Materiel Command
Attn: AMCMA-EE
Washington, D. C. 20315

1 Commanding General
U. S. Army Materiel Command
Attn: AMCRD-TV
Washington, D. C. 20315

1 Commanding General
U. S. Army Missile Command
Attn: AMSMI-RRA, Bldg. 5429
Redstone Arsenal, Alabama 35809

3 CG, U. S. Army Missile Command
Redstone Scientific Info Center
Attn: Chief, Document Section
Redstone Arsenal, Alabama 35809

2 Commanding General
U. S. Army Combat Developments CMD
Combat Support Group
Fort Belvoir, Virginia 22060

1 Commanding General
U. S. Army Combat Developments Command
Attn: CDCMR-E
Fort Belvoir, Virginia 22060

1 Commanding Officer
USACDC CBR Agency
Attn: Mr. N. W. Bush
Fort McClellan, Alabama 36201

1 Commanding Officer
USACDC Artillery Agency
Fort Sill, Oklahoma 73503

3 Commanding General
U. S. Army Test & Evaluation Command
Attn: AMSTE-EL, -FA, -NBC
Aberdeen Proving Ground, Md. 21005

1 Commanding General
U. S. Army Test & Evaluation Command
Attn: NBC Directorate
Aberdeen Proving Ground, Md. 21005

1 Commanding General
U. S. Army Munitions Command
Attn: AMSMU-RE-R
Dover, New Jersey 07801

1 Commanding General
U. S. Army Munitions Command
Operations Research Group
Edgewood Arsenal, Maryland 21010

1 Commanding General
U. S. Army Munitions Command
Attn: AMSMU-RE-P
Dover, New Jersey 07801

1 Commanding Officer
Harry Diamond Laboratories
Attn: Library
Washington, D. C. 20438

1 Commanding General
U. S. Army Natick Laboratories
Attn: AMXRF-EG
Natick, Massachusetts 01760

1 Commanding Officer
Picatinny Arsenal
Attn: SMUPA-TV1
Dover, New Jersey 07801

2 Commanding Officer
Picatinny Arsenal
Attn: SMUPA-VA6, Bldg 59
Dover, New Jersey 07801

1 Commanding Officer
Fort Detrick
Attn: SMUFD-AS-S
Frederick, Maryland 21701

1 Commanding Officer
Fort Detrick
Attn: Technical Library SMUFD-AE-T
Frederick, Maryland 21701

1 Commanding Officer
Edgewood Arsenal
Attn: SMUEA-TSTI-TL
Edgewood Arsenal, Maryland 21010

2 Commanding Officer
U. S. Army Nuclear Defense Laboratory
Attn: Library
Edgewood Arsenal, Maryland 21010

1 President
U. S. Army Artillery Board
Fort Sill, Oklahoma 73503

2 Commanding Officer
Aberdeen Proving Ground
Attn: Technical Library, Bldg 313
Aberdeen Proving Ground, Maryland 21005

1 Commanding Officer
U. S. Army Ballistics Research Labs
Attn: Technical Info Division
Aberdeen Proving Ground, Maryland 21005

2 Commanding Officer
U. S. Army Ballistic Research Labs
Attn: AMXBR-B & AMXBR-1A
Aberdeen Proving Ground, Maryland 21005

1 Commanding Officer
U. S. Army Limited Warfare Lab
Attn: CRDLWL-7C
Aberdeen Proving Ground, Maryland 21005

1 Commanding Officer
USA Garrison
Attn: Technical Reference Division
Fort Huachuca, Arizona 85613

1 Chief, A M. & EW Division
Attn: USAEPG-STEEP-TO
Fort Huachuca, Arizona 85613

1 Commander, U. S. Army Research Office (Durham)
Box CM-Duke Station
Durham, North Carolina 27706

2 USA Security Agency Combat Dev. Actitity
Attn: IACDA-P(T) and 1ACDA-P (L)
Arlington Hall Station, Bldg 420
Arlington, Virginia 22212

1 U. S. Army Security Agency Processing Center
Attn: IAVAPC-R & D
Vint Hill Farms Station
Warrenton, Virginia 22186

1 Technical Support Directorate
Attn: Technical Library
Bldg 3330
Edgewood Arsenal, Maryland 26010

1 Comandant
U.S. Army Chemical Center S School
Micrometeorological Section (Chem. Br.)
Fort McClellan, Alabama 36201

1 Commandant
U.S. Army Air Defense School
Attn: C & S Dept. MSL Science Div.
Fort Bliss, Texas 79916

2 Director
U.S.A. Engineering Waterways Experimental Station
Attn: Research Center Library
Vicksburg, Mississippi 39180

1 CG, Deseret Test Center
Attn: STEPD-TT-ME(S) Meteorological Division
Bldg 103, Soldiers Circle
Fort Douglas, Utah 84113

1 Commanding General
USA CDC Combat Arms Group
Ft. Leavenworth, Kansas 66027

1 Commanding Officer
USA Aviation Materiel Labs
Attn: Technical Director
Fort Eustis, Virginia 23604

1 Director
U.S. Army Advanced Materiel Concepts Agency
Attn: AMXAM
Washington, D. C. 20315

1 Commanding Officer
U.S. Army Combat Developments Command
Communications-Electronics Agency
Fort Monmouth, New Jersey 07703

1 Commandant
U.S. Army Signal School
Attn: Meteorological Department
Fort Monmouth, New Jersey 07703

U.S. ARMY ELECTRONICS COMMAND

1 U.S. Army Liaison Office
MIT. Bldg 26, Room 131
77 Massachusetts Avenue
Cambridge, Massachusetts 02139

1 U.S. Army Liaison Office
MIT-Lincoln Laboratory, Room A-210
P.O. Box 73
Lexington, Massachusetts 02173

1 Headquarters
U.S. Army Combat Developments Command
Attn: CDCLN-EL
Fort Belvoir, Virginia 22060

1 Commanding General
U.S. Army Tank - Automotive Command
Attn: AMSTA-Z, Mr. R. Mc Gregor
Warren, Michigan 48090

1 USAECOM Liaison Office, Stanford University
Solid State Electronics Lab
McCullough Bldg.
Stanford, California 94305

Commanding General
U.S. Army Electronics Command
Fort Monmouth, N.J. 07703

1 AMSEL-EW
1 AMSEL-ME-NMP-PS
2 AMSEL-TD-TI
1 AMSEL-RD-MT
1 AMSEL-XL-D
1 AMSEL-WL-D
1 AMSEL-NL-D
1 AMSEL-KL-D
1 AMSEL-VL-D
3 AMSEL-HL-CT-D
15 AMSEL-BL-FM-P
1 AMSEL-BL-D
1 AMCPM-SL
1 AMCPM-ATMS

OTHER RECIPIENTS

1 Commanding General
U.S. Army Materiel Command
Attn: AMCRD-R (H. Cohen)
Washington, D. C. 20315

1 Institute of Science and Technology
The University of Michigan
P.O. Box 618, (IRIA Library)
Ann Arbor, Michigan 48107

2 NASA Scientific & Technical Info Facility
Attn: Acquisitions Branch (S-AK/DL)
P.O. Box 33
College Park, Maryland 20740

1 Target Signature Analysis Center
Willow Run Labs - Institute of Science 6 Technology
University of Michigan
P. B. Box 618
Ann Arbor, Michigan 48107

1 Battelle-Defender Infor Center
Battelle Memorial Institute
505 King Avenue
Columbus, Ohio 43201

1 Infrared Information and Analysis Center
University of Michigan
Institute of Science and Technology
Box 618,
Ann Arbor, Michigan 48107

3 Vela Seismic Info Center
University of Michigan
Box 618
Ann Arbor, Michigan 48107

1 Head, Atmospheric Sciences Section
National Science Foundation
1800 G Street, N.W.
Washington, D. C. 20550

1 Director, Systems R & D Service
Federal Aviation Administration
800 Independence Ave., S.W.
Washington, D.C. 20590

1 Atmospheric Sciences Library
Environmental Science Services Administration
Silver Spring, Maryland 20910

1 Air Resources Cincinnati Laboratory
% National Air Pollution Control Administration
5710 Wooster Pike
Cincinnati, Ohio 45227

1 U.S. Department of Agriculture
Attn: William A. Main
University of Minnesota
St. Paul, Minnesota 55101

1 Chief, Fallout Studies Branch
Division of Biology and Medicine
Atomic Energy Commission
Washington, D.C. 20545

1 NASA Headquarters
Meteorologv & Soundings Branch (Code SAM)
Space Applications Programs
Washington, D.C. 20546

1 Director
Atmospheric Physics & Chemistry Lab R31
ESSA-Department of Commerce
Boulder, Colorado 80302

1 National Center for Atmospheric Research
NCAR Library, Acquisitions-Reports
Boulder, Colorado 80302

1 0CE, Bureau of Reclamation
Attn: D755, Bldg. 67
Denver, Colorado 80 225

1 National Oceanographic Data Center
Code 2220
Bldg. 160, WNY
Washington, D. C. 20390

Security Classification

DOCUMENT CONTROL DATA - R & D

(Security classification of title, body of abstract and indexing annotation must be entered when the overall report is classified)

1. ORIGINATING ACTIVITY (Corporate author)	2a. REPORT SECURITY CLASSIFICATION
Illinois State Water Survey University of Illinois Urbana, Illinois 61801	UNCLASSIFIED
	2b. GROUP N/A

3. REPORT TITLE

Reflectivity-Rainfall Relationships and Reflectivity Variability Observed with a Hybrid Video Processor

4. DESCRIPTIVE NOTES (Type of report and inclusive dates)

Final Report, 1 February 1969 to 1 February 1971

5. AUTHOR(S) (First name, middle initial, last name)

E. J. Silha and E. A. Mueller

6. REPORT DATE	7a. TOTAL NO. OF PAGES	7b. NO. OF REFS
February 1971	75	18

8a. CONTRACT OR GRANT NO.	9a. ORIGINATOR'S REPORT NUMBER(S)
DAAB07-69-C-0204 b. PROJECT NO.	
c. d.	9b. OTHER REPORT NO(S) (Any other numbers that may be assigned this report) ECOM C-0204-F

10. DISTRIBUTION STATEMENT

This document is subject to special export controls and each transmittal to foreign nationals may be made only with prior approval of CG, US Army Electronics Command, Fort Monmouth, N. J. 07703, ATTN: AMSEL-BL-FM-P

11. SUPPLEMENTARY NOTES	12. SPONSORING MILITARY ACTIVITY
	US Army Electronics Command Fort Monmouth, New Jersey 07703 ATTN: AMSEL-BL-FM-P

13. ABSTRACT

A hybrid video processor was constructed for use in measuring rainfall in convective storms. After the processor was tested in the laboratory, it was used to collect data on two convective storms. Data were collected on 3 days, but on only one day did storm systems occur over the nearby raingage network where comparative rainfall data were available. The data for these storms were analyzed to study relationships between reflectivity and rainfall. An attempt was made to correlate reflectivity with rainfall measured at the ground using a time-space displacement technique for the radar data. A comparison of total water accumulation is also made. Reflectivity variability described by a number of parameters was investigated.

DD FORM 1 NOV 68 1473 REPLACES DD FORM 1473, 1 JAN 64, WHICH IS OBSOLETE FOR ARMY USE.

UNCLASSIFIED

Security Classification

14. KEY WORDS	LINK A		LINK B		LINK C	
	ROLE	WT	ROLE	WT	ROLE	WT
Meteorology Weather radar Precipitation Rainfall rate Viceo processor for radar						